F: TLQUODVR1

Nov 7th 2008

Revised July 2009

Final Revision Aug 2009

(JONSMOD 2008 Paper)

An intercomparison of tidal solutions computed with a range of unstructured grid models of the Irish and Celtic Sea Regions

By

J. Eric Jones, Philip Hall and Alan M. Davies

Proudman Oceanographic Laboratory

Joseph Proudman Building

6 Brownlow Street

Liverpool L3 5DA

England, UK

ABSTRACT

Three finite element codes, namely TELEMAC, ADCIRC and QUODDY are used to compute the spatial distributions of the M_2, M_4 and M_6 components of the tide in the sea region off the west coast of Britain. This region is chosen because there is an accurate topographic dataset in the area, and detailed open boundary M_2 tidal forcing for driving the model. In addition accurate solutions (based upon comparisons with extensive observations) using uniform grid finite difference models forced with these open boundary data exist for comparison purposes. By using boundary forcing, bottom topography, and bottom drag coefficients identical to those used in an earlier finite difference model, there is no danger of comparing finite element solutions for "untuned unoptimised solutions" with those from a "tuned optimised solution". In addition by placing the open boundary in all finite element calculations at the same location as that used in a previous finite difference model and using the same M_2 tidal boundary forcing and water depths, a like with like comparison of solutions derived with the various finite element models was possible. In addition this open boundary was well removed from the shallow water region, namely the eastern Irish Sea where the higher harmonics were generated. Since these are not included in the open boundary forcing their generation was determined by physical processes within the models. Consequently an intercomparison of these higher harmonics generated by the various finite element codes gives some indication of the degree of variability in the solution particularly in coastal regions from one finite element model to another.

Initial calculations using high resolution nearshore topography in the eastern Irish Sea and including "wetting and drying", showed that M_2 tidal amplitudes and phases in the region computed with TELEMAC were in good agreement with observations. The ADCIRC code gave amplitudes about 30 cm lower and phases about 8º higher. For the M_4 tide, in the eastern Irish Sea amplitudes computed with TELEMAC were about 4 cm higher than

ADCIRC on average, with phase differences of order 5º. For the M_6 component, amplitudes and phases showed significant small scale variability in the eastern Irish Sea, and no clear bias between the models could be found. Although setting a minimum water depth of 5 m in the nearshore region, hence removing wetting and drying, reduced the small scale variability in the models, the differences in M_2 and M_4 tide between models remained. For M_6 a significant reduction in variability occurred in the eastern Irish Sea when a minimum 5 m water depth was specified. In this case TELEMAC gave amplitudes that were 1 cm higher and phases 30º lower than ADCIRC on average. For QUODDY in the eastern Irish Sea, average M_2 tidal amplitudes were about 10 cm higher and phase 8º higher than those computed with TELEMAC. For M_4, amplitudes were approximately two centimetres higher with phases of order 15º higher in the northern part of the region and 15º lower in the southern part. For M_6 in the north of the region amplitudes were 2 cm higher, and about 2 cm lower in the south. Very rapid M_6 tidal phase changes occurred in the nearshore regions.

The lessons learned from this model intercomparison study are summarised in the final section of the paper. In addition the problems of performing a detailed model-model intercomparison are discussed, as are the enormous difficulties of conducting a true model skill assessment that would require detailed measurements of tidal boundary forcing, near shore topography and precise knowledge of bed types and bed forms. Such data are at present not available.

1. INTRODUCTION

Although there has been significant progress in recent years in modelling tides and large scale circulation in various geographical areas (e.g. Northwest European Continental Shelf, Davies and Kwong (2000), west coast of Britain, Davies and Jones (1992) (hereafter DJ92), Yellow Sea, Naimie et al. (2001), Irish Shelf (Lynch et al (2003,2004)) the main focus of this work has been outside the very nearshore coastal domain where “wetting and drying”

(Flather and Hubbert 1989, Ip et al 1998) can occur during the tidal cycle. However it must be mentioned that there has been some recent work using high resolution meshes in the nearshore of the Bay of Fundy (Greenberg et al, 2005, Dupont et al 2005). The main reason for this focus on regions where "wetting and drying" does not occur has been the coarse grid nature of these models (e.g. DJ92) which prevented them from resolving these shallow regions. For example shelf wide models of the European continental shelf used a grid resolution of 1/12° and hence could not resolve coastal regions where "wetting and drying" occurred and higher harmonics were generated by non-linear effects. To examine the nearshore generation of higher harmonics, higher resolution limited area finite difference models were developed, for example the 1 km grid model of the eastern Irish Sea used by Jones and Davies (1996) (hereafter JD96). The difficulty of using such limited area models to examine the influence of "wetting and drying" in nearshore regions upon the higher harmonics was that because of the limited extent of the model these harmonics were significant at the open boundary of the model. Hence these harmonics had to be included as open boundary forcing to the model and consequently their distribution over the region was not only influenced by nearshore dynamics but also by open boundary forcing. Consequently the effect of nearshore dynamics could not be examined in detail.

An alternative to using a uniform finite difference grid is to apply an unstructured finite element approach (see Jones (2002), Walters (2005), Greenberg et al (2007) for reviews of the method). This method was used in the English Channel to compare tidal solutions computed with finite difference and finite element models of the area (Werner 1995). However, as the domain of the model was limited higher harmonics were included along the open boundary. In addition there were no appreciable "wetting and drying" areas in the region, hence their effects upon the higher harmonics of the tide could not be investigated.

Consequently although a rigorous model-model and model-data comparison could be performed the solution for the higher harmonics was in part influenced by their distribution along the open boundary. In addition because the model domain had a limited geographic extent the M_2 solution was also in part constrained by the open boundary. In this paper by using a larger domain model, with only M_2 tidal forcing and including "wetting and drying" these problems are to a certain extent minimized (see later). Consequently the higher harmonics are generated entirely by the non-linear processes, in particular momentum advection, quadratic bottom friction and the non-linear term in the continuity equation involving the product of velocity and total water depth (e.g. Davies and Kwong 2000). For a detailed discussion of the generation of higher harmonics the reader is referred to Parker (2007), Walters (1986, 1992). In addition when a nearshore region "wets and dries" over a tidal cycle, the harmonic analysis of the resulting elevation time series contains significant higher harmonics. These arise due to the presence of a Gibbs type effect as drying and subsequent wetting occurs.

In essence this paper extends the work of Werner 1995, by examining a different sea area where the higher harmonics and wetting/drying are important. In addition the sensitivity of the tidal solution in the nearshore region to water depth and finite element resolution is examined in detail. Also, by using a number of finite element models and comparing differences between models and also differences between them and observations, it is possible to illustrate the difficulties in performing a model skill assessment exercise that can reveal "true model" predictive capability in an arbitrary sea region. This problem is discussed in the final part of the paper. These considerations complement the work of Roed et al (1995) who showed how difficult it was to design test cases for model intercomparison.

Recently a finite element tidal model of the west coast of Britain has been developed (Jones and Davies, 2005, hereafter JD05) based upon the application of the TELEMAC code

to solve the finite element equations that describe tidal motion in the region. The TELEMAC code has been used very successfully in other shallow water regions (e.g. Malcherek 2000, Heniche et al 2000, Hervouet 2002, Fernandes et al 2002, 2004) and preliminary calculations (JD05) showed that it could reproduce the major features of the tide off the west coast of Britain without any tuning and using boundary forcing and topography taken from a previous uniform finite difference model. The finite element grid of this model is ideal for examining the effects of nearshore dynamics upon higher harmonics of the tide (Jones and Davies 2007a) for a number of reasons. The most important of these is that the model's open boundary is well removed from the shallow water region, namely the eastern Irish Sea where "wetting and drying" occurs and higher harmonics are generated. Consequently, the model is only forced by the M_2 tide and the higher harmonics are generated solely within the region. In addition the model has high resolution (Fig. 1) in the shallow eastern Irish Sea (Fig. 2a,b) where higher harmonics are important. Also, there is a comprehensive tidal data set, including the higher harmonics for model validation and an accurate solution from a limited area high resolution (1 km) finite difference model of the region, for comparison purposes.

The objective of this paper is to examine to what extent a range of finite element codes, namely TELEMAC (Hervouet 2002), ADCIRC (e.g. Hench and Luettich 2003, Luettich and Westerink 1995) and QUODDY (e.g. Naimie et al 2001) can calculate the higher harmonics of the M_2 tide in the eastern Irish Sea, and the sensitivity of the solution to changes in nearshore water depth. In addition small scale variations of the tide in the near coastal region are used to examine the sensitivity of the solution to grid resolution. Although tidal calculations are only performed with the M_2 tidal forcing and other calculations (e.g. the three dimensional models of Jones and Davies (1996), Lynch et al (2003,2004)) included more constituents which can influence the tide (see later discussion) the model intercomparisons are very revealing. In addition as shown by Aldridge and Davies (1993)

there is significant spatial variability in bed types and bed forms over the eastern Irish Sea, which besides the presence of other tidal constituents appreciably influences tidal damping in the region. These uncertainties and the fact that the main emphasis of the paper is to compare the various model solutions justifies the use of the M_2 tidal forcing only. In order to compare models, in all calculations the same water depth distribution and bottom friction coefficient was used. As shown by Nicolle and Karpytchev (2007) there is a good case for a spatially variable friction close to the coast. However to perform "like with like" comparisons a constant value was used here. This is consistent with earlier finite difference calculations. In addition open boundary tidal forcing was the same in all calculations and taken from that used by DJ92. The open boundary conditions used in DJ92 were based on limited offshore observations in the region and tidal solution from larger domain models (Kwong et al 1997). Although there may have been some inaccuracy in this boundary forcing they were shown to give an accurate tidal solution in the region when used to force a finite difference model. An alternative used by Lynch et al (2003) is to use assimilation into a model to derive off shore boundary conditions. However, problems in accuracy of tidal data, particularly that of off shore data (see later) and any numerical bias in the assimilation model may lead to a bias in this open boundary forcing. In essence in order to derive a truly unbiased accurate offshore set of tidal data requires precise off shore tidal measurement at locations which have a major influence upon the computed tidal solution. An example of how to use a model to determine the critical tidal measurements that are required in offshore regions is given in Davies (1976). However, in the case of the present model, this would prove to be an expensive measurement exercise. Hence in all calculations, tidal forcing was identical to that used in DJ92. Consequently models were not tuned to give an accurate tidal solution, by adjusting open boundary input, friction or depths, and hence differences in model solution reflected model dynamics.

The fact that all the finite element models were run with the same topography, M_2 tidal open boundary forcing and same bottom friction, taken from an earlier finite difference model of the region, ensures that the forcing and dissipation had not been adjusted to optimize the solution for a particular finite element code. Consequently there was no "built in" bias to favour one particular finite element model. In addition the model-model and model-data intercomparisons are a "true" test of the variability in solutions of each of the finite element models, rather than the usual approach where a model is "tuned" to give the "best fit" to a set of observations.

As will be shown later by not "tuning" the models it is possible to determine the true variability in solutions computed with a range of finite element models. In addition model bias to under/over predict a particular constituent can be assessed. By including or omitting near coastal shallow water regions the extent to which these influence the higher harmonics and hence the degree to which accurate nearshore topography has to be measured and must be resolved can be assessed. In addition the intercomparison exercise illustrates the major problems in doing model-model and model-data intercomparisons, and the enormous difficulties of doing a "rigorous model skill" assessment exercise.

The form of the hydrodynamic equations solved with these various finite element codes is presented in the next section. Solutions from the various codes are given in subsequent sections together with details of their sensitivity to water depth variation, and their variability in nearshore regions. Major conclusions from the study are presented in the last section of the paper, where the difficulties in doing a "true model skill assessment" are discussed.

2. HYDRODYNAMIC EQUATIONS

Since the focus of the study is tidal elevation, then it is sufficient to solve the two dimensional vertically integrated hydrodynamic equations, details of which are given in DJ92

and JD96 and will not be repeated here. As the west coast of Britain model spans a range of latitudes (Fig. 1a,b) then spherical coordinates were used, although the region was not sufficiently large to require the addition of tidal potential forcing. Since these equations contain all the non-linear terms necessary to generate the higher harmonics of the tide, then in principle given accurate topography and an appropriate form of bottom friction, together with accurate tidal forcing, they should be able to reproduce the higher tidal harmonics.

The same water depth distribution, finite element grid (Fig. 2) and M_2 tidal open boundary forcing taken from the finite difference model described in DJ92 which yielded an accurate M_2 tidal distribution in the region, were used in the TELEMAC, ADCIRC and QUODDY calculations. Consequently differences in solution arise from differences in the various codes. Solutions were generated from initial conditions of zero elevation and motion at t = 0, by integrating forward in time over seven tidal cycles and harmonically analysing the final cycle for the M_2, M_4 and M_6 constituents. Preliminary calculations showed that because of significant frictional dissipation in the region a sinusoidal solution, that was independent of the initial conditions was established within six tidal cycles. For this reason the seventh tidal cycle was harmonically analysed and used in the comparisons. At closed boundaries the normal component of velocity was zero. In addition the horizontal gradient normal to the coast of alongshore velocity was set to zero, giving a perfect lateral slip condition.

3. NUMERICAL SOLUTION

3.1 Grid Generation

The underlying water depths describing the domain and open boundary tidal description originate from the finite difference models of DJ92 and JD96 and were used to generate the finite element grid of JD05 allowing a like with like comparison with these earlier models. Previous calculations with JD05 showed that an optimal M_2 tidal solution in the region was obtained using a mesh refinement based on water depth such that the ratio

between element size and $(gh)^{½}$ was constant, with g acceleration due to gravity and h water depth. This approach was applied here with the identical water depths used in JD05, to give grid G3AX (Fig. 2). In this grid the maximum size of element had a side length of order 5 km and occurred in deep water, with nearshore elements of order 0.5 km. As the model water depths included nearshore values that were above mean sea level, "wetting and drying" occurred during the tidal cycle. To examine to what extent the tidal solution, in particular the higher harmonics was influenced by this, a second mesh was generated (G3AX5M) in which all water depths shallower than 5m were replaced by a 5 m minimum water depth. This revised set of water depths was then used to generate a new grid G3AX5M using the identical criteria, namely $(gh)^{1/2}$, as that for grid G3AX. Consequently in deep water nodal locations were the same, but in shallow water the two meshes were slightly different. Calculations (Table 1) were performed using all the codes on both meshes, except for the version of QUODDY used here which did not allow for "wetting and drying" and was therefore only run on grid G3AX5M. By this means the influence of including accurate nearshore water depths and the associated "wetting and drying" upon the accuracy of the tide could be determined. We have recently learned from a reviewer that a version of QUODDY now exists (Greenberg et al 2005) that allows for "wetting and drying". However as the main aim here is to show to what extent "wetting and drying" influences a solution this can be illustrated with the TELEMAC and ADCIRC results.

Although a number of techniques exist in the literature to generate an optimal mesh for a given problem and area (e.g. Hagen et al 2001, 2002, Legrand et al 2006, 2007 and the review of Greenberg et al 2007) these methods were not used here, where the main aim was to compare a number of finite element solutions using the same mesh

3.2 TELEMAC

3.2.1 Calculations including detailed nearshore topography, Grid G3AX (Calc 1)

In an initial calculation (Calc 1, Table 1) tides were computed using the TELEMAC code and grid G3AX. Since detailed results and discussions of the co-tidal charts are given elsewhere (JD05) only the main points are presented here. Comparisons with observations at coastal and offshore tide gauges in the eastern Irish Sea (see Fig. 3, and JD05 for exact locations) for the M_2, M_4 and M_6 tidal elevation amplitude and phase are given in Tables 2a,b and c.

The computed M_2 cotidal chart (Fig. 4a(i)) is characterized by a rapid increase in amplitude in shallow water regions such as the Bristol Channel and eastern Irish Sea. It is important to note that for clarity of contour annotation these co-tidal charts are derived by gridding the detailed output from the finite element model. Consequently there is some loss of resolution in the near shore region. Within the North Channel of the Irish Sea the model reproduces the tidal distribution found in limited area high resolution models of the region (Davies et al 2001) and derived from measurements (George 1980). In addition the amphidromic point in the western Irish Sea, and the overall distribution of the tidal amplitude and phase in the Irish Sea is in good agreement with cotidal charts based on observations (Robinson 1979). A detailed point by point comparison with measurements at coastal and offshore gauges in the Eastern Irish Sea (Table 2a) shows that on average there is good agreement although at some locations tidal amplitude is slightly over-estimated by about 10 cm, with phase of order 5° too high. As the accuracy of the instrument and length of the record used to derive this harmonic analysis varies from location to location, with typically a 2 month record from an offshore tide gauge and 12 months from a coastal gauge then providing error bars on the observational data is very difficult. This is a major consideration in any skill assessment exercise. However as the main aim of the paper is a model-model intercomparison, then the changes in solution given in the various tables are a true measure of inter-model variability.

At a number of shallow water coastal gauges for example Hilbre (location E), Barrow (where there are three gauges at locations Y, Z and AA, in close proximity to each other, see Fig. 3), Morecambe (BB) and Fleetwood (CC), there appears to be some difference between observed and computed values, despite the fact that the finite element mesh has high resolution in these regions of order 50m. To understand this, values at nearby nodal positions a distance Δ from the observational point were examined (Table 3a).

It is apparent that at Hilbre at the nearest nodal point (Δ = 1.1 km, h = 9.6 m), h_c = 307 cm, g_c = 310° (compared with h_o = 292, g_o = 317°) that is 15 cm too high and 7° too low. At an equivalent (Δ = 1.1 km) point in shallower water h = 2 m, h_c = 269 cm, g_c = 308°, namely 39 cm too low, and 9° too low. This suggests that despite the high resolution mesh in the region, there is significant spatial variability in the tide from one mesh point to the next. At nodes slightly farther away, namely Δ = 1.3 and 1.8 km, water depths are 16.2 m and 2.3 m, with the higher tidal amplitude occurring in the deeper water (Table 3a) where frictional effects are less. Despite the change in amplitude, the phase changes very little from one point to the next, suggesting that at this location the mesh is sufficiently fine to resolve tidal phase if not tidal amplitude.

At Barrow RI (location Y), at the two closest nodes the water depth is zero compared to mean sea level and significant "wetting and drying" occurs. This leads to an appreciable reduction in M_2 tidal amplitude compared to the observed. At other nearby locations where the water depth is non-zero both amplitude and phase are in good agreement with observations. This suggests that the water depth at the two nearest points in the model may be incorrect, or there is a local deeper water channel that is not resolved in the model. At Barrow HP (location Z), again at the point where the water depth is zero, the M_2 tidal amplitude is under-predicted, with amplitude being slightly over-predicted and phase under-predicted at the other locations, suggesting slight errors in local water depth.

At Barrow HS (location AA), at the three nearest points the water depth is non zero with the model tending to slightly over-predict amplitude and under-predict phase, although there is little variation from one nodal point to another. However, at Morecambe there is appreciable spatial variability in tidal amplitude over the three nearest nodes, although water depth changes by less than 1 m between them. This suggests that the mesh is insufficiently fine to resolve the tidal variability in the region. As at other locations, in very shallow water h = 0.9 m, the tidal amplitude is significantly reduced.

Spatial variability at Fleetwood is comparable to that found at Morecambe, suggesting that the mesh is not sufficiently fine and water depths are not available with sufficient accuracy to obtain a smooth convergent solution in these near coastal regions. In essence the M_2 tidal variation in these nearshore regions is comparable to the mesh resolution of the model. Obviously the model mesh could be continuously refined in the near shore region until a convergent solution was obtained. However, without precise knowledge of water depths in the coastal area, which can change between storm events, and accurate knowledge of bed types and bedforms which influence frictional dissipation in the region (Aldridge and Davies 1993) it is unlikely that continuous mesh refinement will guarantee increased model accuracy. As the main aim here is a model intercomparison on a fixed mesh, then an indication of solution variability for that mesh in the near shore is all that is required. Obviously, in a skill assessment exercise of a model's true predictive capability this will be limited by our knowledge of near shore conditions.

The computed M_4 cotidal chart (Fig. 4b) shows the M_4 tidal amplitude, which was zero on the model's open boundary, increasing over the Celtic Sea to a maximum of 10 cm in the southern part of the Irish Sea. The computed M_4 amplitude decreases from this maximum to a minimum to the west of the Isle of Man (Fig. 4b). This spatial variability is found in observations and shelf wide finite difference numerical models (Davies and Kwong 2000). In

the shallow eastern Irish Sea the M_4 amplitude increases rapidly as the shallow coastal region is approached (Fig. 4b). On average the M_4 tide in the eastern Irish Sea is computed with a comparable accuracy to the higher resolution (1 km grid) limited area (eastern Irish Sea only) finite difference model of JD96. This level of agreement suggests that the TELEMAC model is correctly reproducing the physical aspects of the processes generating the M_4 tide. In JD96 although the finite difference model yielded an accurate solution this was in fact in part due to the specification of the M_4 tide along the open boundary of that limited area model.

Although in general the M_4 tide is adequately reproduced, it is evident that at certain coastal locations there are some significant errors (Table 2b). Considering the near coastal locations used previously for the M_2 tide, it is evident that at Hilbre the M_4 tidal amplitude varies by only 4 cm over the four nearest nodes, although there is a significant variation in phase from 158° to 228° (Table 3b). This is in marked contrast to the M_2 tide where the phase was essentially uniform but the amplitude varied (Table 3a).

At Barrow RI in regions where the water depth was zero, and "wetting and drying" occurred the amplitude was significantly larger than found in the observations (Table 3b). At these locations the M_2 tidal elevation was decreased below the observed (Table 3a) due to excessive energy going into the M_4 tide. At the two locations close to Barrow RI where "wetting and drying" did not occur, M_4 tidal amplitude agreed well with the observed, Table 3b, although the phase was under-estimated. Similarly at Barrow HP, at the location of zero water depth, tidal amplitude was over-estimated (Table 3b). At other sites close to Barrow HP computed and observed amplitude and phase were in good agreement, with phase showing only a small spatial variation. This suggests that at this site the M_4 is well resolved on the mesh.

At Barrow HS computed amplitude and phase show only small scale variability, with amplitude showing good agreement with observed, although the phase was under-estimated

(Table 3b). Significant spatial variability exists in the computed M_4 tide at Morecambe which is related to the variability found in the M_2 tide (Table 2b). At Fleetwood, at the shallow water nodes, the amplitude of the M_4 tide is again over-estimated (Table 3b) with a corresponding decrease in the M_2 tide (Table 3a) due to "wetting and drying" transferring energy into the higher harmonics. As discussed previously this suggests inaccurate water depths or a deep channel not resolved by the model. At the node 2.3 km from the tide gauge, M_4 amplitude is in reasonable agreement with observations, although the phase is under-predicted. These detailed M_4 comparisons in shallow water explain why the M_2 tide at some nodes is significantly below the observed, with an associated over-estimate of the M_4 tide.

The computed M_6 cotidal chart (Fig. 4c) shows a rapid increase in tidal amplitude in shallow water due to an increase in bottom friction. In the Liverpool Bay region there is a gradual increase as the water shallows, with a more rapid increase as the Cumbrian coast is approached. The spatial changes in M_6 are due to local decreases in water depth, with a rapid increase in regions where "wetting and drying" occurs (see later). Similar spatial variability with changes in water depth are found in the observed M_6 tide.

Comparisons at various ports (Table 2c) shows that at a number of locations the model significantly overpredicts tidal amplitude. The reason for this can be understood by examining the spatial variability of the tide in the region of the observational point (Table 3c). Considering initially Hilbre, it is evident that at Δ = 1.1 km in very shallow water h = 2 m, h_c = 21 cm compared with h_o = 2 cm. However, slightly farther away Δ = 1.3 km, and h = 16.2m, or nearer Δ = 1.1 km, h = 9.6 m, h_c is reduced to 7 or 8 cm. As for the M_4 tide, the M_6 tide shows significant spatial variability over short distances.

At Barrow RI in regions that "wet and dry", namely h = 0 m, the amplitude, although not the phase, is in reasonable agreement with observation. However at nearby deeper water nodes there are significant errors in both amplitude and phase. Similarly at Barrow HP at

nodes in deeper water locations the tidal amplitude is larger than at nodes in the shallow water, with a significant difference in phase error. At Barrow HS, all adjacent nodes are in deeper water, and have comparable values, of order 6 cm, which although higher is in reasonable agreement with the observed 3 cm, although the phase is about 35° too low, suggesting a local change that is not resolved in the model. Although there are large phase changes of order 35° in M_6, the fact that a phase change of 87° represents only a one hour time shift for this constituent, does put these errors into perspective compared with the M_2 tide.

Comparable M_6 tidal amplitudes are found at all nodes at Morecambe, although there is significant spatial variability in the phase. In addition tidal amplitude is over-estimated. This suggests that there are local changes that are not resolved in the model. Similar spatial variability is found at Fleetwood, again suggesting a lack of resolution.

From the M_4 and M_6 cotidal charts (Fig. 4b(i), 4c(i)) it is evident that their amplitude and phase change very rapidly in shallow water, particularly in the eastern Irish Sea in regions such as the Solway estuary and Morecambe Bay. A detailed examination of the tidal distribution in these regions (Fig. 4b(ii), 4c(ii)) clearly shows that more detailed coastal resolution is required, with an associated enhanced refinement of the mesh. As discussed previously the contours shown here were derived by gridding finite element output and do not reflect the high resolution of the finite element grid (Fig. 2) in the near shore region. For the M_2 tide the present resolution appears adequate, although the extent to which it and the shallow water constituents are influenced away from the coastline by details of nearshore topography and the presence of "wetting and drying" is not clear. This problem is examined in the next section.

3.2.2. Calculation involving under-resolved nearshore topography Grid G3AX5M (Calc 2)

To examine to what extent the solution away from the nearshore region is influenced by near coastal water depths that are normally not resolved in coarse grid models, or not available with sufficient spatial coverage or accuracy, the previous calculation was repeated with a minimum water depth of 5 m. This also meant that "wetting and drying" did not take place and hence its influence on the solution was removed. Although changing the water depth distribution produced a slightly different grid in the near shore region (namely grid G3AX5M, Table 1), since this is related to $(gh)^{½}$ (see earlier discussion), away from the coastline the nodal distribution was as previously.

Comparison of the model wide computed cotidal chart (not shown) (derived with this modified grid (Calc 1M, Table 1)) with that derived previously (Fig. 4a(i)(ii)) did not reveal any significant differences outside the Irish Sea region. However, within the Irish Sea, in particular the eastern Irish Sea away from the nearshore region there was on average an increase in tidal amplitude (compare Figs. 4a(ii) and 5a(ii)) due to the removal of shallow water coastal regions where significant energy dissipation occurred (Davies and Kwong 2000) and energy was transferred to higher harmonics. It is evident from a comparison of Figs. 4a(ii) and 5a(ii) that in the nearshore region of the eastern Irish Sea the effect of setting the minimum water depth to 5 m is to remove the small scale variability in the M_2 tidal amplitude found with realistic water depths. This gives rise to a much smoother variation in the co-amplitude lines comparable to those found in coarse grid models (Davies and Kwong 2000).

Comparing computed values in Table 2a (Calc 1 and Calc 1M) it is evident that at offshore gauges S, T, U (Fig. 3) the removal of shallow water in near coastal regions leads to a decrease in M_2 tidal amplitude of the order of about 5 cm, although no significant change in phase. A larger decrease of order 8 cm occurs at coastal gauges in the Liverpool Bay region (e.g. gauges B, F) with little phase change. In very shallow regions (e.g. Morecambe BB)

amplitude increases by about 20 cm, although as discussed previously in the case of the G3AX grid, this depends upon the location of the nodal point.

To determine to what extent spatial variability in shallow regions is influenced by grid and water depth change, the same locations used previously were considered (Table 3a). Since the mesh distribution has changed, then both Δ and h are different from those given previously (Table 3a), although again nearest locations are used. Considering initially Hilbre (Table 4a, Calc 1M) it is evident that at this location, although water depth changes significantly from one node to another, the effect of imposing a minimum depth of 5 m is that there is only a small variation in tidal amplitude and phase from one node to another, compared to previously where realistic water depths were applied. This shows that with a minimum depth of 5 m the mesh is adequate to resolve the computed M_2 tide. A similar result is found at Barrow RI and HP, although at Barrow HS there is some small scale variability. As illustrated in Tables 3a and 4a, setting a minimum depth of 5 m significantly increases tidal amplitude (Table 4a) above that found previously using realistic depths at locations where these were below 5 m. At Morecambe and Fleetwood, water depths at nearby nodes (Table 3a) were appreciably less than 5 m, and hence the effect of specifying a 5 m minimum is to produce a region of constant water depth (Table 4a) and increased tidal amplitude. Despite the water depths at Morecambe having h = 5 m, the tidal amplitude varies by 4 cm, and phase by 4° over relatively short distances suggesting that a further mesh refinement is required despite the constant water depth in the region. In addition when more realistic water depths are used, the spatial variability increases, with a significant reduction compared to observations in very shallow water. This suggests that as the grid is refined more detailed accurate nearshore topography that can resolve deeper channels is also required.

Considering the M_4 component of the tide, as for the M_2 tide outside the Irish Sea (not shown) there is not a significant difference between the M_4 tide computed using mesh G3AX and G3AX5M. However in the eastern Irish Sea (compare Figs. 4b(ii) and 5b) the M_4 tidal amplitude is significantly reduced when a minimum h = 5 m is used. This average reduction in M_4 tidal amplitude is evident from a comparison at gauges in the eastern Irish Sea (compare Calcs 1 and 1M in Table 2b). At offshore gauges in deeper water (locations S, T, U) it is evident from Table 2b that amplitude has reduced by 4 cm on average, with phase increasing by 10° to 15°. In Liverpool Bay, at gauges I, Q, R, the amplitude change is small, of order 1 cm, with phase change of 15°. However further north at offshore gauge V the amplitude is reduced by 6 cm, with phase increasing by over 30°. Similarly at coastal gauges in this region namely H and K (Fig. 2b) the amplitude is reduced from 12 cm (Calc 1) to 6 cm (Calc 1M) (cf, observed 12 cm at H), and 13 cm (Calc 1) to 7 cm (Calc 1M) (cf, observed 13 cm) at K. This confirms what is shown in Figs. 4b(ii) and 5b, that although the M_4 tide is affected over the whole eastern Irish Sea, the largest difference is in the northern part of the region. Although amplitude is reduced on average it is evident from Table 2b, that at some locations (e.g. Heysham, Hilbre, Barrow HP) it has increased. To examine this it is necessary to consider the small scale variability close to the tide gauge (Table 4b). As for the M_2 tide the effect of using a minimum water depth of 5m, is to remove a significant amount of the spatial variability (Table 4b) of the M_4 tide in the region of the tide gauge (see Hilbre, Barrow RI, Barrow HP and Fleetwood in Table 4b) compared to previously (Table 3b). This tends to lead to a reduction at nodes where previously “wetting and drying” occurred and an increase elsewhere. However, at locations such as Barrow HS more spatial variability is introduced, with an associated increase in M_4, reducing the agreement of the nearest node average and the observation. Similarly at Morecambe the use of a minimum water depth of 5 m leads to a significant increase in M_4 amplitude. This suggests that, as for M_2, as water depth spatial

variability is reduced, so the mesh resolution can be coarser, although the error in the computed tide is enhanced giving rise to inaccuracies in the model.

For the M_6 tide the distribution of co-amplitude and co-phase lines outside the Irish Sea (not shown) computed with mesh G3AX5M (Calc 1M) is comparable to that given in Fig. 4c(i). However, within the eastern Irish Sea particularly in the northern and nearshore region there are appreciable differences (compare Figs. 4c(ii) and 5c). In particular in the calculation with a minimum water depth of 5 m the spatial variability is smoother, and there is not a rapid increase close to the coast.

Comparisons at both offshore and coastal gauges in the eastern Irish Sea (Table2c, Calc 1 and Calc 1M) show that at offshore gauges (e.g. locations Q to U) there is little change in amplitude although phase changes by a few degrees. This is to be expected since the M_6 tide is generated by local bottom friction and influenced locally by "wetting and drying". Since these effects at offshore locations are not appreciably changed between meshes G3AX and G3AX5M, then this is to be expected. However, in nearshore regions there are significant differences in the solutions.

From calculations 1 and 1M in Tables 3c and 4c, as for M_2 and M_4, specifying a minimum water depth, at all locations appreciably reduces the spatial variability in the solution. However, at Morecambe the amplitude still changes significantly over relatively short distances, suggesting that a finer mesh is required. In addition the M_6 amplitude is appreciably larger than the measured value. This suggests that the large value found in both solutions is not due to "wetting and drying" or the effect of harmonically analysing a discontinuous time series, but arises from non-linear effects in particular bottom friction which may be incorrectly formulated in these shallow regions.

3.3 ADCIRC

3.3.1 *Calculations including detailed nearshore topography, Grid G3AX (Calc 3)*

In order to quantify (Tables 2a-c) and examine the spatial variability of the differences between the tides computed using TELEMAC and ADCIRC, differences in amplitude and phase between the M_2, M_4 and M_6 constituents computed with TELEMAC and ADCIRC are given in Figs. 6a-c. Since both models are forced with identical open boundary input, then it is evident that in the region of the open boundary, the two solutions are the same. However, the location of the amphidromic point off the south-east corner of Ireland is slightly further north in the calculation with ADCIRC compared to the TELEMAC calculation. This gives rise to a positive difference in the region to the north of the amphidrome and negative to the south, as shown in the difference plot (Fig. 6a). In addition there are phase differences in the region of the amphidromic point. Similarly in the region of the North Channel there are differences in the tidal distribution computed with each of the models, as shown in the distribution of differences (Fig. 6a). The differences in the two solutions increase within the Irish Sea, particularly in the eastern Irish Sea, where the tidal amplitude computed with ADCIRC is of the order of 30 cm below that computed with TELEMAC, with phase 8º higher (Fig. 6a). These differences are clearly evident (compare Calcs 1 and 2, Table 2a) at the coastal gauges given in Table 2a, with ADCIRC having a tendency to underpredict the tide in shallow regions, although TELEMAC gave good agreement. In terms of M_2 phases, it is evident from Table 2a and Fig. 6a, that ADCIRC computed phases of order 8º higher than TELEMAC. This gave rise to slightly better agreement with the observed phase than that found with TELEMAC. The reason for this difference in amplitude and phase in the eastern Irish Sea is that at offshore gauges V, U, S, T in the eastern Irish Sea (see Fig. 3b for gauge locations) the M_2 tidal amplitude derived from TELEMAC (Calc 1, Table 2a) was significantly (of order 10 cm) higher than the observed whereas for ADCIRC it was about 20 cm lower. In addition the phase is of the order of 8º higher at these offshore gauges. This suggests that it is not just differences in numerical

damping in the nearshore region between the two models that produce differences in the agreement at coastal gauges, but also the M_2 tidal propagation over the whole domain. The fact that the M_2 tidal solution from TELEMAC is in better agreement at eastern Irish Sea coastal gauges than ADCIRC (compare Calcs 1 and 2 in Table 2a) is in part due to the fact that this model tended to overpredict the tide at the offshore gauges V, U, S and T and in essence both models have a tendency to overdamp tidal energy in the shallow eastern Irish Sea. This may in part be due to the fact that no attempt was made to optimize bottom friction in this region or elsewhere in the model.

In terms of differences in the computed M_4 co-tidal chart, it is evident (Fig. 6b) that these are small outside the eastern Irish Sea. This is to be expected since Fig. 4b(i) shows that the M_4 tide is largest in the eastern Irish Sea. In the southern half of the eastern Irish Sea it is apparent (Fig. 6b) that the M_4 tidal amplitude computed with TELEMAC is larger than that determined with ADCIRC, whereas in the north of the region the M_4 amplitude from ADCIRC is slightly larger. In addition, away from the very near coastal region in the northern half of the eastern Irish Sea, ADCIRC computes phase of order 10^o higher than TELEMAC. However, in the southern half of the eastern Irish Sea the phase difference between the two solutions is small (Fig. 6b). These differences are apparent at offshore gauges T and V (Table 2b). This may also be seen at northern coastal gauges e.g. H and K, where M_4 amplitude from ADCIRC exceeds that from TELEMAC, whereas at southern gauges e.g. E and O, TELEMAC M_4 amplitudes exceed those from ADCIRC (see Table 2b, Calcs 1 and 2). Also, phases from TELEMAC exceed those from ADCIRC. In view of the fact that TELEMAC gives a larger M_2 tide in the eastern Irish Sea than ADCIRC, and M_4 is mainly produced by M_2 interacting with itself, suggests that M_4 computed with TELEMAC (Calc 1) should exceed that computed with ADCIRC (Calc 2). This is found on average over the whole Irish Sea, but does not explain the difference between the northern and southern

regions of the eastern Irish Sea. One possibility why this difference occurs in M_4, is that M_2 interacts with M_4, to give M_6, takes some energy from the M_4 tide. Although the amplitude of the M_6 tide, even in shallow water is small compared with the M_2 tide (typically of order 10 cm compared with 2 m) and consequently it is not important in terms of total tidal elevation, it is a valuable indicator of a model's accuracy in shallow water. To examine to what extent M_2 and M_4 interaction produce M_6 in the eastern Irish Sea it is useful to consider the distribution of the M_6 tide in the eastern Irish Sea. However, contours of the difference in the M_6 tidal amplitude computed with TELEMAC and ADCIRC (not shown) did not show substantial differences except in the nearshore region, due to the small (of order 1 cm in the north eastern Irish Sea and 5 cm in the south eastern Irish Sea, see Fig. 4c) amplitude of the M_6 tide. Comparison of M_6 tidal amplitudes (Calcs 1 and 2) at coastal gauges where there was an appreciable signal (Table 2c) showed that there was a bias for the M_6 computed from TELEMAC to exceed that from ADCIRC. This probably arises because the M_2 tide in shallow water computed with TELEMAC exceeds that derived with ADCIRC. However, this does not explain the differences in the M_4 distribution. The above analysis of M_2 interacting with itself to give M_4, and subsequent M_2 and M_4 interaction to give M_6 is based upon an energy cascade from lower to higher frequencies. In practice just as M_2 interacts with itself to give a tidal residual, M_2 can interact with M_4 and M_6 to transfer energy to lower frequencies (see Walters 1986, 1992) although the amplitude of the lower frequencies generated by this process will be small.

In terms of M_6 phases, it is evident from Table 2c that there is significant spatial variability in both computed and observed phases in coastal regions. Also, there does not appear to be a consistent difference between M_6 phases computed with TELEMAC and ADCIRC in these regions.

As was found in the M_2 tidal solution computed with TELEMAC there is significant spatial variability in the M_2 tidal amplitude computed with ADCIRC in the region surrounding a coastal gauge (see Calc, 2 Table 3a).

In essence the high spatial variability found in the TELEMAC calculation of the M_2 amplitude (Calc 1, Table 3a) at nodal points adjacent to shallow water ports is also found in ADCIRC (Calc 2, Table 3a). Also, as found on average throughout the model domain, the amplitude computed with ADCIRC (Calc 2) is below that found in TELEMAC (Calc 1). In addition phases computed with ADCIRC are very slightly (of order 3^o on average, Table 3a) larger than those computed with TELEMAC. However, both models give consistent phases and show that the phase does not change appreciably at nodal points near the gauges.

For the M_4 component of the tide, the ADCIRC calculation shows comparable spatial variability in tidal amplitude with nodal location (Calc 2, Table 3b) to that found with TELEMAC (Calc 1, Table 3b). However, as discussed previously in terms of the eastern Irish Sea M_4 tidal distribution, the M_4 amplitude computed with ADCIRC, is less than that due to TELEMAC (compare Calcs 1 and 2 in Table 3b). As suggested previously because M_4 is generated by the non-linear interaction of M_2 with itself, then a reduction in M_2 amplitude will reduce the M_4 amplitude. The significant spatial variability found in the M_4 phase computed with TELEMAC also occurs with ADCIRC. Although ADCIRC on average gives a larger phase than TELEMAC, at some nodal locations the phase is below that computed with TELEMAC (compare Calcs 1 and 2 in Table 3b). This suggests that there is significant small scale variability in the solutions computed with these models.

This small scale variability is also found in the M_6 tidal amplitude computed with ADCIRC (Calc 2, Table 3c). For the M_6 component at most locations there are significant differences between Calcs 1 and 2, and these differences vary appreciably from one point to another. However, at some locations, namely Barrow HS and Morecambe both models give

comparable amplitudes although there are appreciable phase differences from one node to another, suggesting that there are differences in the model's ability to reproduce phase variations for the higher harmonics in near coastal regions.

3.3.2 *Calculation involving under-resolved nearshore topography, Grid G3AX5M (Calc 2M)*

To examine to what extent the inclusion of complex nearshore topography contributes to the differences in tidal solutions computed with ADCIRC and TELEMAC, the ADCIRC code was used to compute the tide using the G3AX5M grid. This solution is then compared with that using TELEMAC on the same grid (Calc 1M, Table 1). As a detailed discussion of the influence of near shore topography upon the tidal solution has been presented for the TELEMAC code, only brief details in terms of ADCIRC will be given here.

Contours of the difference in M_2 tidal amplitude and phase between Calc 1M and Calc 2M (Fig. 7a), outside the eastern Irish Sea, show similar distributions to those found with detailed topography (Fig. 6a). However, in the eastern Irish Sea in the near coastal region the small scale variability in these differences is reduced (compare Figs 6a and 7a).

From Table 2a, it is clear that the reduction in M_2 tidal amplitude and change in phase at eastern Irish Sea coastal gauges found between Calcs 1 and 2, is also found between Calcs 1M and 2M. On average the reduction in M_2 amplitude computed with ADCIRC, using grid G3AX5M is comparable to that found with G3AX, namely of the order of 30 cm, with phase changing by the order of 8º. In essence this is consistent to that found between TELEMAC and ADCIRC using grid G3AX, suggesting that each model responds in the same way to the removal of shallow water regions.

For the M_4 tide the difference outside the eastern Irish Sea between TELEMAC and ADCIRC using grid G3AX5M (Fig. 7b) and the higher resolution grid G3AX (Fig. 7a) mainly occurs in the region of the M_2 amphidromic point off the southwest corner of Ireland.

The change in position of this amphidromic point between the solutions influences the distribution of the M_2 tide along the west coast of Wales (Fig. 6a). When the water depth in this region changes between grids G3AX5M and G3AX, this influences the local generation of M_4 in the region leading to an increased difference between M_4 amplitude computed with TELEMAC and ADCIRC using grid G3AX5M than G3AX (compare Figs. 6b and 7b). However, in the eastern Irish Sea the difference in M_4 tidal amplitude computed with TELEMAC and ADCIRC is reduced (compare Figs. 6b and 7b). However the phase difference in the solutions in the north of the eastern Irish Sea increases slightly.

A detailed comparison of M_4 solutions (Table 2b) suggests that although the two models still give appreciably different M_4 solutions using grid G3AX5M, they show consistent differences in the solution using high resolution (G3AX grid) or smooth topography (G3AX5M) in the nearshore region.

For the M_6 component of the tide the difference plot (not presented) together with point by point comparison of ADCIRC solutions (Table 2c) shows that as for the TELEMAC code at offshore gauges S, T, U, V changing from grid G3AX to G3AX5M does not appreciably influence the amplitude, but does affect the phase. However the change in phase going from G3AX to G3AX5M is different in the two models. A detailed analysis (not presented) shows appreciable differences in phase between TELEMAC and ADCIRC even when M_6 is computed using grid G3AX5M where there is no small scale variation in topography and "wetting and drying" does not occur. This suggests that for M_6 the computed solution derived from each model is significantly different. This may in part be due to a lack of grid resolution in the nearshore region even when the smooth topography is used.

To finalize the comparison of the TELEMAC and ADCIRC solutions using grid G3AX5M it is useful to look at the spatial variability at nodes surrounding various nearshore gauges (Table 4a). As with the TELEMAC solution once a minimum water depth of 5 m is

specified in the nearshore region of the eastern Irish Sea, the spatial variability at nodes surrounding an observational point for all tidal constituents is significantly reduced (see Calc 2M in Tables 4a-c). However, as discussed previously there are significant differences in the solutions computed with TELEMAC and ADCIRC even with this smooth idealized nearshore topography.

3.4 QUODDY

As shown previously, even when smoother nearshore topography (namely grid G3AX5M) is used in the calculations, and "wetting and drying" does not occur there are significant differences in tidal solutions computed with TELEMAC and ADCIRC. Although QUODDY, as used here, does not include "wetting and drying" and hence cannot be run on grid G3AX, it is still useful to examine the tidal solution on grid G3AX5M, and see how this compares with other solutions.

Difference plots between the TELEMAC and QUODDY solutions (Calcs 1M and 3M) for the M_2 tide (Fig. 8a) and point comparisons in the eastern Irish Sea (Table 2a, Calcs 1M and 3M) show that on average the tidal amplitude computed with QUODDY exceeds that determined with TELEMAC.

From Fig. 8a it is apparent that the amphidromic point off the southeast coast of Ireland computed with QUODDY is farther north than that computed with TELEMAC. Also a detailed comparison of cotidal charts showed that the amphidrome computed with QUODDY was slightly to the east of that derived with TELEMAC. This gives rise to tidal amplitudes computed with QUODDY that are lower than TELEMAC in the region to the north of the amphidromic point (Fig. 8a). A similar distribution of the difference between the models was found with ADCIRC (see Fig. 6a) However the difference between the M_2 tidal amplitudes computed with TELEMAC and QUODDY decreases to the west of the Isle of Man, with QUODDY giving larger amplitudes in the eastern Irish Sea than TELEMAC (Fig.

8a). This is significantly different than that found with ADCIRC , where the difference between TELEMAC and ADCIRC increased in the eastern Irish Sea (Fig. 6a). One reason for these different distributions is that the difference between TELEMAC and ADCIRC given in Fig. 6a, is based on mesh G3AX, but Fig. 8a uses mesh G3AX5M. However since Fig. 6a is comparable to Fig. 7a, based on mesh G3AX5M, this difference appears to arise from using QUODDY rather than ADCIRC, rather than differences in mesh.

It is evident from Table 2a (comparison of Calcs 1M and 3M) that at locations on the western side of the eastern Irish Sea in deeper water e.g. locations Douglas and offshore gauge S that the M_2 tidal amplitude and phase computed with QUODDY, exceed those computed with TELEMAC by about 5 cm and 8º (see Fig. 8a). This difference on average has a tendency to increase as the water shallows, giving on average in the coastal region a difference in amplitude of 10 cm and phase of 5º to 10º (Fig. 8a). This suggests that the M_2 tidal solution in shallow water computed with QUODDY is slightly less damped than in TELEMAC.

For the M_4 component of the tide (Fig. 8b) it is evident that in some regions outside the eastern Irish Sea, particularly close to the amphidromic point off the southeast coast of Ireland there are some appreciable differences in M_4 computed with TELEMAC and QUODDY (Fig. 8b). The distribution of these differences and their magnitudes is quite different from that found in the TELEMAC/ADCIRC intercomparison (Fig. 7b) suggesting that although all three models are forced with the same M_2 tide, there are differences in the numerical representation of the processes generating the M_4 tide. These are most likely to be in the numerical formulation of the non-linear momentum terms that move energy towards shorter waves and higher frequencies, and the implicit or explicit momentum diffusion terms which control this movement and stabilize the solution by removing energy at short waves. To fully identify these terms and their differences in the various models would require a

range of calculations using the codes to solve the simple advection problem in an idealized domain, possibly with and without the linearization of non linear terms. Such an exercise is outside the scope of this paper. However, from a comparison of Figs. 7b and 8b it is evident that although ADCIRC underestimates M_4 amplitude compared with TELEMAC (Fig. 7b), in the case of QUODDY the computed M_4 amplitude is larger in near coastal regions than that computed with TELEMAC (Fig. 8b). In both calculations there was a tendency for the M_4 phase to be overpredicted in the northern part of the region, compared to TELEMAC.

For the M_4 component of the tide, Fig. 8b and Table 2b, show that on average in the shallow water region of the eastern Irish Sea the QUODDY code (Calc 3M) gives a slightly higher amplitude of order 2 cm, than TELEMAC (Calc 1M). As discussed previously this is probably due to the slightly higher M_2 tidal amplitude in the region. However, in some very shallow water locations where TELEMAC computes a very large M_4 amplitude e.g. Heysham and Morecambe, the amplitude computed by QUODDY is significantly increased (e.g. Heysham Calc 1M, h_c = 39 cm, Calc 3M, h_c = 50 cm and Morecambe Calc 1M, h_c = 66 cm, Calc 3M, h_c = 83 cm). This increase in M_4 amplitude computed with QUODDY in shallow near coastal regions is particularly strong in the Barrow region as shown in Fig. 8b. Although there is consistent agreement in the amplitude between solutions computed with both codes, there is some variation in the phase close to the coast. It is not clear what is the reason for these differences between the M_4 solution in shallow water computed with TELEMAC and QUODDY.

For the M_6 component the cotidal chart (not presented) shows that outside the eastern Irish Sea there are some differences in the M_6 amplitude computed with TELEMAC and QUODDY, in particular in the western Irish Sea, to the north of the M_2 amphidromic point. This is different to that found with ADCIRC, although in general, outside the nearshore region the M_6 tide is small. In the eastern Irish Sea M_6 amplitude differences between

TELEMAC and QUODDY are appreciably larger (Table 2c), than those between TELEMAC and ADCIRC. In addition the M_6 amplitude computed with QUODDY changes very rapidly in the region of Barrow.

From Table 2c, there does not appear to be a consistent difference between the M_6 computed with TELEMAC and that derived with QUODDY. However, as found for the M_4 tide at locations where M_6 is large e.g. Birkenhead and Morecambe, that computed with QUODDY is significantly larger than that derived with TELEMAC.

It is evident from Table 4a, (Calc 3M) that as in Calcs 1M and 2M, when the minimum water depth is set at 5 m there is significantly less spatial variability in the QUODDY solution than found with TELEMAC or ADCIRC using realistic depths (e.g. Calcs 1 and 2). As discussed previously, at all these shallow water locations the M_2 amplitude from QUODDY (Calc 3M) exceeds that from TELEMAC, which has the closest agreement with observed shallow water amplitudes. This is in contrast to that found with ADCIRC (Calc 2M) where the amplitude is underpredicted. In terms of phase, that computed with QUODDY (Calc 3M) is very slightly (of order 1^o or 2^o on average) higher than that computed with TELEMAC.

For the M_4 component of the tide, as for M_2, using a minimum water depth removes the spatial variability in the region of the nodes found with G3AX (Calc 3M, Table 4b). In addition at most tidal locations the M_4 amplitude computed with QUODDY (Calc 3M) is not appreciably different from that determined by TELEMAC (see Calcs 1M and 3M in Table 4b). However, as discussed in connection with Table 2b, at locations such as Morecambe where TELEMAC gives a large M_4 tide (Calc 1M), there is a tendency for QUODDY to compute a larger amplitude than TELEMAC (compare Calcs 1M and 3M, Table 4b). For M_4 phase, on average that computed with QUODDY is of the order 10^o below that computed with TELEMAC (compare Calcs 3M and 1M, Table 4b).

Considering the M_6 component of the tide, as found for TELEMAC and ADCIRC, there is significantly less variability at nodal positions surrounding the observational point when the minimum depth is set at 5 m. In addition as discussed previously, at a number of shallow water locations, namely Barrow RI, Barrow HP and Morecambe, QUODDY has a tendency to overpredict the M_6 tidal amplitude compared with TELEMAC and ADCIRC, and at Barrow HS , it underpredicts the phase (Table 4c). However at other locations e.g. Fleetwood, the amplitude is in good agreement with the other solutions, although the phase is too low (see Table 4c). The reason for this is not clear, although it is evident from Table 4c, that even when a minimum depth is set at 5 m, there is significant variability in the M_6 solution computed with the various models.

CONCLUDING REMARKS

Three finite element codes, namely TELEMAC, ADCIRC and QUODDY with two different finite element meshes, namely G3AX, which resolves the detailed nearshore eastern Irish Sea topography, and G3AX5M which does not, have been used to compute the spatial distribution of the M_2, M_4 and M_6 tides over the west coast of Britain. This region was chosen because an existing finite difference uniform coarse grid (7 km) model solution of the region existed, in addition to a solution from a fine resolution (1 km) eastern Irish Sea model. Also a detailed observational data set was available over the region for comparison purposes, particularly in the eastern Irish Sea where higher harmonics of the M_2 tide were produced.

In all calculations the same open boundary forcing and water depth distribution to that used in earlier finite difference calculations was employed. By this means all finite element models were forced in the same way and had identical water depths. Consequently there was no bias in the solution obtained by adjusting the input or water depths in one model compared to another. Also the same bottom friction coefficient, that was constant over the whole region, and bottom stress formulation was used in all calculations. This however is a major

approximation, in that as shown by Aldridge and Davies (1993) there is significant variation in bed types and bed forms over the eastern Irish Sea which should be taken into account in any attempt at a highly accurate simulation of the tides. In addition to this as shown in JD96, other tidal constituents in particular S_2, N_2, K_1 and O_1 need to be included in order to get the correct level of frictional dissipation. Consequently a "true model-model and model-data intercomparison" has been performed in the sense that no optimization was performed, rather than the "conventional skill assessment" where a model-data comparison is performed after optimizing the model. However, as discussed previously this falls short of a "true skill assessment" of the predictive capabilities of a range of finite element models, but is somewhat different to the "conventional skill assessment" of a single model where a model-data comparison is performed after the model has been optimized in terms of friction etc. In addition by using a range of finite element models, with identical forcing and water depths any bias in a particular model for example to over/under predict amplitude and phase in a consistent manner could be identified and the model adjusted for future use. For example an under-prediction of amplitude and over-prediction of phase could indicate enhanced numerical dissipation that could be corrected by using a less dissipative algorithm. However, as shown in the calculations and discussed later such simple biases between models did not occur, due to the complex physical nature of tidal propagation and the high non-linearity of the solution in this region.

For example initial calculations with TELEMAC and ADCIRC showed that even for the M_2 tide with a detailed topographic data set there were differences in amplitude and phase over the whole region. These appeared to arise from the fact that the two models gave slightly different locations for the amphidromic point off the southeast coast of Ireland. This gave rise to, on average a 30 cm difference in amplitude and 8^o difference in phase for the M_2 tide in the eastern Irish Sea computed with the two models, with the TELEMAC solution in

this region in closer agreement with observations. However, as found in previous finite difference calculations (DJ92, Davies and Kwong 2000) the location of amphidromic points in the interior of large domain models is sensitive to small changes in open boundary forcing. This is true in the present case, but since the open boundary forcing was taken from an accurate earlier finite difference model (DJ92) no adjustment had been made in any finite element calculation. Consequently although the significant differences between TELEMAC and ADCIRC in the eastern Irish Sea might at first sight be attributed to differences in numerical damping in shallow water, in practice it is probably due to small subtle differences in model formulation, which slightly moves the position of the M_2 tidal amphidromic point.

This difference in M_2 in the eastern Irish Sea subsequently feeds into the local M_4 in this region. Thus, a consequence of the larger M_2 tidal amplitude computed with TELEMAC than ADCIRC is that the M_4 amplitude is also larger in the eastern Irish Sea. This suggests that to get a correct M_4 tide, the model must be able to accurately compute the M_2 tide, not only in the region of the M_2 amphidrome, but as it propagates into the eastern Irish Sea. At first sight, differences in M_4 distributions between models in the eastern Irish Sea may be attributed to numerical differences in the non-linear momentum advection terms, since these are primarily responsible for M_4 generation. Certainly this would be so for the idealized case of a one dimensional solution of a tidal wave propagating into shallower water. In such a case any reduction in higher harmonics could be readily attributed to artificial viscosity introduced into the finite element representation of momentum advection. However as shown here in a “true model-model assessment” the reason can be more complex and relate to “far field” errors in M_2 tidal propagation.

For M_6 both TELEMAC and ADCIRC exhibit significant spatial variability in the near coastal region over relatively short distances. In addition neither model exhibits good agreement with observations which also show appreciable small scale variability. One reason

for this, as discussed in JD96, is that in order to get an accurate M_6 tide it is essential to have an accurate description of bottom friction and this requires the inclusion of other tidal constituents (namely S_2, N_2, K_1 and O_1). However, even without these constituents, and ignoring the observations that are generally small which could be prone to error, it is evident from a comparison of TELEMAC and ADCIRC M_6 computations, that there are appreciable differences in the solutions and there is no clear trend in this difference. This is a different situation from that found for the M_2 and M_4 tide where there were consistent large scale differences in the solution. This suggests that these differences in M_6 may arise from small scale nearshore topographic variations in water depth that are unresolved even on the fine nearshore eastern Irish Sea grid used here, or due to differences in model formulation. However, even when a minimum nearshore depth of 5 m is used in the calculation, it is apparent that there are changes in the M_6 tide computed with TELEMAC, ADCIRC and QUODDY. In an idealized calculation such as that involving tidal propagation in a one dimensional shallowing estuary, then changes in the M_6 tide between different models can in part be related to how they parameterize and discretize the bottom friction term. However, as shown here, because of differences in the M_2 and M_4 tides compared with the different models, the reason is more complex. However, some of the difference in the M_6 solution must arise from differences in model formulation, and the possibility of under-resolving this component of the tide in the nearshore region. In addition the absence of other tidal constituents and the use of a single friction coefficient over the whole domain must be a source of error. As shown by Aldridge and Davies (1993) and Davies and Lawrence (1995) bed types vary significantly over the eastern Irish Sea, suggesting an appreciable variation in bottom drag coefficient (Nicolle and Karpytchev 2007). To this end, further calculations are in progress with the use of additional tidal constituents, bed type dependent friction and enhanced nearshore resolution. For a large number of nearshore processes (e.g. Levasseur et

al 2007), such as sediment transport and the spread of pollutants it is essential to have a correct description of both the M_2 component of the tide and its higher harmonics as well as the tidal residual (Jones and Davies 2007b). To this end further work is in progress to improve the tidal description of the eastern Irish Sea.

The calculations presented here, clearly show that a model skill assessment based upon model-data comparison after the model has been optimized in one particular region may not be a true indication of model accuracy in other regions. In addition by comparing results from three models that have not been optimized for the area examined, it is clear that small differences in the location of the M_2 tidal amphidromic point can feed through to significant differences in the M_2, M_4 and M_6 tides in shallow regions. These differences are primarily caused by "far field" effects (i.e. small inaccuracies in location of the M_2 amphidrome) rather than differences in model algorithms, that might at first sight be thought to be the principal factor. This clearly shows the limitations of interpreting local deficiencies in a model containing a range of physical processes and covering a wide domain, in terms of results that are found using very idealized calculations of limited domains.

In terms of a rigorous "skill assessment" of a number of models this suggests that besides accurate validation data, detailed accurate open boundary conditions are required at sufficient locations (see Davies (1976) for a discussion of this) to provide accurate and unbiased model forcing. In addition a detailed accurate topographic data set, containing not only water depths, but bed types and forms is required, particularly in the near shore region, bearing in mind that close to the coast these can change between major storm events. At present no such comprehensive data sets exist, and the cost of making the necessary measurement would be large. In essence the model intercomparison exercise presented here, reinforces the conclusions reached by Roed et al. (1995), concerning the difficulties of formulating and carrying out rigorous model intercomparisons.

ACKNOWLEDGEMENTS

The origin of the TELEMAC system is EDF-LNHE and is therefore ©EDF-LNHE. The authors are indebted to R.A. Smith for help in preparing diagrams, E Ashton and L. Parry for typing the paper. The authors are indebted to two anonymous reviewers for valuable comments particularly concerned with “model skill assessment”.

REFERENCES

Aldridge, J.N. and Davies, A. M. (1993) A high resolution three-dimensional hydrographic tidal model of the eastern Irish Sea. Journal of Physical Oceanography, 23, 207-224.

Davies, A. M. (1976) A numerical model of the North Sea and its use in choosing locations for the deployment of offshore tide gauges in the JONSDAP'76 oceanographic experiment. Deutsche Hydrographische Zeitschrift, 29, 11-24.

Davies, A.M. and Jones, J.E. (1992) A three dimensional model of the M_2, S_2, N_2, K_1 and O_1 tides in the Celtic and Irish Sea. Progress in Oceanography, 29, 197-234.

Davies, A.M. and Lawrence, J. (1995) Modelling the effect of wave-current interaction on the three-dimensional wind driven circulation of the eastern Irish Sea. Journal of Physical Oceanography, 25, 29-45.

Davies, A.M. and Kwong, S.C.M. (2000) Tidal energy fluxes and dissipation on the European Continental Shelf. Journal of Geophysical Research, 105, 21969-21989.

Davies, A.M., Hall, P., Howarth, M.J., Knight, P. and Player, R. (2001) A detailed comparison of measured and modeled wind driven currents in the North Channel of the Irish Sea. J. Geophys. Res., 106, 19,683-19,713.

Dupont, F., Hannah, C.G., and Greenberg, D.A. (2005) Modeling the sea-level of the upper Bay of Fundy, Atmosphere-Ocean 43(1) 33-47.

Fernandes, E.H.L., Dyer, K.R., Moller, O.O. and Niencheski, L.F.H. (2002) The Patos lagoon hydrodynamics during an El Nino event (1998). Continental Shelf Research, 22, 1699-1713.

Fernandes, E.H.L., Marino-Tapia, I. Dyer, K.R. and Moller, O.O. (2004) The attenuation of tidal and subtidal oscillations in the Patos Lagoon estuary. Ocean Dynamics, 54, 348-359.

Flather, R.A. and Hubbert, K.P. (1989) Tide and surge models for shallow water – Morecambe Bay revisited, pg. 135-166 in Modeling Marine Systems, Vol 1, CRC Press, Boca Raton, Florida, USA.

George, K.J. (1980) Anatomy of an amphidrome. Hydrographic Journal, 18, 5-12.

Greenberg, D.A., Shore, J.A., Page, F.H., and Dowd, M. (2005) Finite element circulation model for embayments with drying intertidal areas and its application to the Quoddy region of the Bay of Fundy. Ocean Modelling 10, 211–231.

Greenberg, D.A., Dupont, F., Lyard, F.H., Lynch, D.R. and Werner, F.E. (2007) Resolution issues in numerical models of oceanic and coastal circulation. Continental Shelf Research, 27, 1317-1343.

Hagen, S., Westerink, J., Kolar, R., Horstmann, O. (2001) Two dimensional unstructured mesh generation for tidal models. International Journal for Numerical Methods in Fluids, 35, 669-686.

Hagen, S.C., Horstmann, O., Bennett, R.J. (2002) An unstructured mesh generation algorithm for shallow water modeling. International Journal of Computational Fluid Dynamics, 16(2), 83-91.

Hench, J.L. and Luettich, R.A. (2003) Transient tidal circulation and momentum balances at a shallow inlet. Journal of Physical Oceanography, 33, 913-932.

Heniche, M., Secretin, Y., Boudreau, P. and Leclerc, M. (2000) A two-dimensional finite element drying-wetting shallow water model for rivers and estuaries. Advances in Water Resources, 23, 359-372.

Hervouet, J-M (2002) TELEMAC modeling system: an overview. Hydrological Processes, 14, 2209-2210.

Ip, J.T.C., Lynch, D.R. and Friedrichs, C.T. (1998) Simulation of estuarine flooding and dewatering with application to Great Bay, New Hampshire. Estuarine Coastal and Shelf Science, 47, 119-141.

Jones, J.E. (2002) Coastal and shelf-sea modelling in the European context. Oceanography and Marine Biology: an Annual Review, 40, 37-141.

Jones, J E and Davies, A M (1996) A high resolution three dimensional model of the M_2, M_4, M_6, S_2, N_2, K_1, and O_1 tides in the eastern Irish Sea. Estuarine Coastal and Shelf Science 42, 311-346.

Jones, J.E. and Davies, A.M. (2005) An intercomparison between finite difference and finite element (TELEMAC) approaches to modelling west coast of Britain tides. Ocean Dynamics, 55, 178-198.

Jones, J.E. and Davies, A.M. (2007a) On the sensitivity of computed higher tidal harmonics to mesh size in a finite element model. Continental Shelf Research, 27, 1908-1927.

Jones, J.E. and Davies, A.M. (2007b) On the sensitivity of tidal residuals off the west coast of Britain to mesh resolution. Continental Shelf Research, 27, 64-81.

Kwong, S.C.M., Davies, A.M. and Flather, R.A. (1997) A three dimensional model of the principal tides on the European Shelf. Progress in Oceanography, 39, 205-262.

Legrand, S. Deleersnijder, E., Hanert, E., Legat, V. and Wolanski, E. (2006) High-resolution, unstructured meshes for hydrodynamic models of the Great Barrier Reef, Australia. Estuarine, Coastal and Shelf Science, 68, 36-46.

Legrand, S. Deleersnijder, E., Delhez, E. and Legat, V. (2007) Unstructured, anisotropic mesh generation for the Northwestern European continental shelf, the continental slope and the neighbouring ocean. Continental Shelf Research, 27, 1344-1356.

Luettich, R.A. and Westerink, J.J. (1995) Continental shelf scale convergence studies with a barotropic tidal model. In: Lynch D.R. and Davies A.M. (ed). Quantitative skill

assessment for coastal ocean models, published American Geophysical Union, pp. 349-311.

Levasseur, A., Shi, L., Wells, N.C., Purdie, D.A. and Kelly-Gerreyn, B.A. (2007) A three-dimensional hydrodynamic model of estuarine circulation with an application to Southampton Water, U.K. Estuarine Coastal and Shelf Science, 73, 753-767.

Lynch, D.R., Naimie, C.E., and Smith, K.W. (2003) Tidal Atlas for the Irish Shelf Seas. Numerical Methods Laboratory Report NML-03-7, Dartmouth College, Hanover NH USA. http://www-nml.dartmouth.edu/Publications/internal_ reports/NML-03-7.

Lynch, D.R., Smith, K.W., and Cahill, B. (2004) Seasonal Mean Circulation on the Irish Shelf -- A Model-Generated Climatology, Continental Shelf Research 24:18, 2215-2244.

Malcherek, A. (2000) Application of TELEMAC-2D in a narrow estuarine tributary. Hydrological Processes, 14, 2293-2300.

Naimie, C.E., Blain, C.A., Lynch, D.R. (2001) Seasonal mean circulation in the yellow Sea – a model-generated climatology. Continental Shelf Research, 21, 667-695.

Nicolle, A. and Karpytchev, M. (2007) Evidence for spatially variable friction from tidal amplification and asymmetry in a shallow semi-diurnal embayment: the pertuis Breton Bay of Biscay, France. Continental Shelf Research, 27, 2346-2356.

Parker, B.B. (2007) Tidal Analysis and Prediction, NOAA Special Publication NOS CO-OPS3. Silver Spring, Maryland. Library of Congress Control Number 2007925298.

Robinson, I.S. (1979) The tidal dynamics of the Irish and Celtic Seas. Geophysical J.R. Astron. Soc., 56, 159-197.

Roed, L.P., Hackett, B., Gjevik, B. and Eide L.I. (1995) a review of the Metocean Modeling Project (MOMOP) Part 1: Model Comparison Study, pg. 285-305. In Quantitative

Skill Assessment for Coastal ocean Models, ed. D.R. Lynch and A.M. Davies, published American Geophysical Union.

Walters, R.A. (1986) A finite element model for tidal and residual circulation. Commun. Appl. Numer. Methods, 2, 393-398.

Walters, R.A. (1992) A three-dimensional, finite element model for coastal and estuarine circulation. Continental Shelf Res., 12, 83-102.

Walters, R.A. (2005) Coastal ocean models: two useful finite element methods. Continental Shelf Research, 25, 775-793.

Werner, F.E. (1995) A field test case for tidally forced flows: a review of the tidal flow forum pg. 269-284 in Quantitative Skill Assessment for Coastal Ocean Models, ed. D.R. Lynch and A.M. Davies, published American Geophysical Union.

CAPTIONS FOR FIGURES

Fig. 1: (a) Topography and place names over the whole region, (b) expanded plot of the topography and local place names in the eastern Irish Sea.

Fig. 2: Finite element grid G3AX of the west coast of Britain.

Fig. 3: Location of eastern Irish Sea gauges used in the comparisons.

Fig. 4: Computed (Calc 1, Grid G3AX) (a) M_2 tide, (b) M_4 tide and (c) M_6 tide over (i) whole region and (ii) eastern Irish Sea.

Fig. 5: As Fig. 4 but only in the eastern Irish Sea, computed (Calc 1M), using the grid G3AX5M.

Fig. 6: Computed difference between tidal solutions derived using TELEMAC and ADCIRC using grid G3AX (namely Calc 1 – Calc 2) for (a) M_2, (b) M_4 tide and (c) M_6 tide over (i) whole region and (ii) eastern Irish Sea.

Fig. 7: As Fig. 6, but using grid G3AX5M (namely Calc 1M – Calc 2M), but only for M_2 and M_4 and for the whole shelf.

Fig. 8: As Fig. 6, but using grid G3AX5M and the difference between TELEMAC and QUODDY (namely Calc 1M – Calc 3M), but only for M_2 and M_4 and for the whole shelf.

Table 1: Summary of Calculations

CALC	CODE	GRID
1	TELEMAC	G3AX
2	ADCIRC	G3AX
1M	TELEMAC	G3AX5M
2M	ADCIRC	G3AX5M
3M	QUODDY	G3AX5M

Table 2a: Comparison of observed amplitude (cms) and phase (degrees) (h_0, g_0) and computed (h_c, g_c), at the M_2 tidal frequency for various ports from Calcs 1 to 3M.

Point	Port	Observed		Calc 1		Calc 2		Calc 1M		Calc 2M		Calc 3M	
		h0	g0	hc	gc	hc	gc	hc	gc	hc	gc	hc	gc
A	Barrow	308	331	311	329	224	326	297	328	268	333	320	329
B	Birkenhead	311	323	310	313	270	316	301	317	272	321	325	320
C	Douglas	230	326	235	314	206	321	231	314	200	322	233	323
D	Heysham	315	325	317	318	282	324	315	323	283	331	337	327
E	Hilbre	292	317	307	310	266	312	308	311	271	313	323	313
F	Liverpool	312	323	308	313	269	317	299	318	272	321	326	320
G	Formby	312	315	305	307	267	312	306	308	268	314	317	313
H	Hestan	275	339	274	322	246	332	270	324	242	335	283	335
I	Liverpool Bay	262	315	306	306	265	311	305	307	266	312	316	312
J	Ramsay	262	328	250	315	217	322	243	315	212	322	248	324
K	Workington	273	332	279	319	250	328	275	319	246	329	287	328
L	Wylfa Head	206	300	225	289	192	293	223	290	191	293	216	299
M	Liverpool (G.D.)	307	321	308	312	268	315	305	314	271	317	324	316
N	Llandudno	267	308	281	299	242	304	279	300	240	304	284	305
O	New Brighton	306	318	308	312	269	315	305	313	271	317	322	316
P	Amlwch	235	305	245	293	211	298	242	294	210	297	239	302
Q	OSTG	290	315	308	307	266	311	305	308	267	312	317	312
R	Queens Channel	296	316	307	307	266	311	306	308	267	313	317	313
S	STD Irish Sea	235	317	251	305	217	311	248	304	215	311	250	312
T	STN 10	262	318	277	306	240	312	271	307	236	313	278	313
U	STN 34	263	324	274	312	241	320	270	313	239	321	280	321
V	STN 35	255	332	266	319	236	328	258	320	228	329	265	329
W	Creetown	233	342	255	327	231	335	255	325	226	334	263	334
X	Conwy	241	318	217	299	191	302	272	299	236	303	279	304
Y	Barrow RI	306	329	156	322	136	325	301	329	272	334	324	331
Z	Barrow HP	292	327	308	324	273	325	301	329	272	334	324	330
AA	Barrow HS	297	325	301	314	267	321	300	314	266	323	314	322
BB	Morecambe	308	326	283	329	239	334	307	334	283	341	334	337
CC	Fleetwood	305	326	191	322	191	320	311	322	278	326	332	323

Table 2b: Comparison of observed amplitude (cms) and phase (degrees) (h_0, g_0) and computed (h_c, g_c), at the M_4 tidal frequency for various ports from Calcs 1 to 3M.

Point	Port	Observed		Calc 1		Calc 2		Calc 1M		Calc 2M		Calc 3M	
		h0	g0	hc	gc	hc	gc	hc	gc	hc	gc	hc	gc
A	Barrow	19	252	38	207	24	293	42	237	29	246	37	228
B	Birkenhead	23	217	28	154	14	150	19	186	14	211	27	210
C	Douglas	6	233	7	177	7	182	3	216	2	226	2	239
D	Heysham	20	243	11	194	10	115	39	223	35	241	50	218
E	Hilbre	20	203	27	165	13	156	31	179	23	172	30	164
F	Liverpool	23	214	30	154	16	153	19	183	16	201	27	205
G	Formby	25	235	19	156	15	151	20	164	17	169	24	160
H	Hestan	12	280	12	176	15	189	6	228	4	285	8	292
I	Liverpool Bay	21	196	20	151	13	150	20	167	16	167	22	160
J	Ramsay	7	237	10	163	11	173	4	181	3	180	3	195
K	Workington	13	253	13	173	16	181	7	213	4	247	7	241
L	Wylfa Head	4	182	2	160	1	216	1	190	1	283	11	296
M	Liverpool (G.D.)	22	202	33	157	18	155	27	178	20	183	30	180
N	Llandudno	12	181	13	138	10	138	10	151	9	145	10	131
O	New Brighton	23	198	32	158	18	155	27	179	20	183	29	180
P	Amlwch	6	185	6	144	4	152	4	159	3	160	3	343
Q	OSTG	17	196	21	152	14	150	20	168	16	169	22	161
R	Queens Channel	17	197	21	154	14	150	21	168	17	170	23	162
S	STD Irish Sea	6	201	8	149	7	152	5	157	4	157	4	149
T	STN 10	16	199	13	150	10	151	9	165	8	167	10	161
U	STN 34	11	217	13	156	13	161	8	180	7	187	10	181
V	STN 35	11	248	11	168	14	179	4	201	3	222	4	223
W	Creetown	30	274	30	208	26	207	10	185	6	194	6	200
X	Conwy	26	216	39	223	30	237	10	133	9	128	10	111
Y	Barrow RI	30	274	66	284	54	290	44	241	34	253	44	235
Z	Barrow HP	26	216	31	203	10	118	44	240	31	251	40	232
AA	Barrow HS	16	200	14	180	10	149	15	214	15	224	23	212
BB	Morecambe	11	217	33	244	9	249	66	250	61	263	83	245
CC	Fleetwood	11	248	63	261	45	278	36	220	25	227	35	205

Table 2c: Comparison of observed amplitude (cms) and phase (degrees) (h_0, g_0) and computed (h_c, g_c), at the M_6 tidal frequency for various ports from Calcs 1 to 3M.

Point	Port	Observed		Calc 1		Calc 2		Calc 1M		Calc 2M		Calc 3M	
		h0	g0	hc	gc	hc	gc	hc	gc	hc	gc	hc	gc
A	Barrow	3	49	13	41	19	97	5	263	6	292	10	231
B	Birkenhead	5	321	15	323	12	345	14	319	11	310	17	241
C	Douglas	1	354	1	72	1	299	1	28	1	346	1	134
D	Heysham	2	11	8	300	7	286	11	251	10	272	15	223
E	Hilbre	2	33	7	331	5	2	9	3	8	18	6	21
F	Liverpool	5	322	14	327	11	354	14	321	10	319	16	247
G	Formby	5	11	6	331	5	341	6	313	6	349	3	343
H	Hestan	-	-	1	113	2	169	4	341	1	49	9	27
I	Liverpool Bay	-	-	6	311	5	341	5	319	6	353	3	4
J	Ramsay	-	-	2	110	2	201	1	42	2	160	3	67
K	Workington	2	325	1	173	2	202	4	324	1	16	8	28
L	Wylfa Head	-	-	1	205	1	269	1	188	1	247	2	79
M	Liverpool (G.D.)	5	349	13	326	9	353	11	329	8	339	7	279
N	Llandudno	2	356	3	289	3	314	3	275	3	314	2	342
O	New Brighton	5	329	13	325	9	352	11	326	8	337	7	276
P	Amlwch	-	-	1	248	1	304	2	223	1	288	1	266
Q	OSTG	4	14	6	315	5	345	6	318	6	352	2	358
R	Queens Channel	3	18	6	318	5	343	6	320	6	352	3	352
S	STD Irish Sea	1	354	2	287	2	311	2	279	2	315	1	329
T	STN 10	3	335	3	300	3	319	3	289	3	326	1	355
U	STN 34	1	7	2	310	2	304	3	307	2	325	2	26
V	STN 35	1	234	1	119	2	171	3	357	2	119	6	44
W	Creetown	5	117	12	66	7	88	4	28	3	144	8	58
X	Conwy	6	22	21	11	19	13	3	264	3	308	2	320
Y	Barrow RI	5	117	4	170	3	83	8	245	7	276	15	221
Z	Barrow HP	6	22	10	16	3	299	7	250	7	281	13	222
AA	Barrow HS	3	355	6	320	6	317	5	257	5	285	7	210
BB	Morecambe	1	7	17	24	15	339	15	207	13	229	26	198
CC	Fleetwood	1	234	8	103	14	67	9	258	7	278	10	218

Table 3a: Spatial variability of computed M_2 tidal elevations h_c (cm) and phase g_c (degrees) with distance Δ (km) between nearest nodal points and observational points from calcs 1 and 2. Also given is the local water depth h(m).

Port	Observed				Calc 1		Calc2	
	h0	g0	Δ	h(m)	hc	gc	hc	gc
Hilbre	292	317	1.1	9.6	307	310	266	312
			1.1	2	269	308	244	311
			1.3	16.2	313	308	267	312
			1.8	2.3	287	308	257	312
Barrow RI	306	329	1	0	156	322	136	325
			1	0	155	314	137	325
			1.9	9.1	308	324	273	325
			2.2	6.4	310	327	224	325
Barrow HP	292	327	1	9.1	308	324	273	325
			1.1	5.9	307	324	272	325
			1.6	3.3	308	328	271	325
			2.1	0	156	322	136	325
Barrow HS	297	325	0.6	6.2	301	314	267	321
			2	5.4	309	316	270	321
			2.1	8	305	312	267	320
Morecambe	308	326	0.6	3	283	329	239	334
			1.6	3.7	309	324	266	330
			2	2.9	257	333	236	335
			2	0.9	207	330	196	330
Fleetwood	305	326	0.3	0.9	191	322	191	320
			0.9	1	212	320	190	323
			1	1.5	252	313	229	320
			2.3	9.6	316	316	276	320

Table 3b: Spatial variability of computed M_4 tidal elevations h_c (cm) and phase g_c (degrees) with distance Δ (km) between nearest nodal points and observational points from calcs 1 and 2. Also given is the local water depth h(m).

Port	Observed				Calc 1		Calc2	
	h0	g0	Δ	h(m)	hc	gc	hc	gc
Hilbre	20	203	1.1	9.6	27	165	13	156
			1.1	2	31	228	17	231
			1.3	16.2	27	158	14	159
			1.8	2.3	28	209	12	201
Barrow RI	30	274	1	0	66	284	54	290
			1	0	62	276	54	291
			1.9	9.1	31	203	10	118
			2.2	6.4	32	206	25	296
Barrow HP	26	216	1	9.1	31	203	10	118
			1.1	5.9	29	207	10	115
			1.6	3.3	25	211	10	123
			2.1	0	66	284	54	290
Barrow HS	16	200	0.6	6.2	14	180	10	149
			2	5.4	15	175	10	144
			2.1	8	14	165	11	152
Morecambe	11	217	0.6	3	33	244	9	249
			1.6	3.7	19	182	8	156
			2	2.9	30	244	10	258
			2	0.9	48	295	38	306
Fleetwood	11	248	0.3	0.9	63	261	45	278
			0.9	1	61	258	45	274
			1	1.5	43	263	29	277
			2.3	9.6	13	165	9	146

Table3c: Spatial variability of computed M_6 tidal elevations h_c (cm) and phase g_c (degrees) with distance Δ (km) between nearest nodal points and observational points from calcs 1 and 2. Also given is the local water depth h(m).

Port	Observed				Calc 1		Calc2	
	h0	g0	Δ	h(m)	hc	gc	hc	gc
Hilbre	2	33	1.1	9.6	7	331	5	2
			1.1	2	21	35	17	36
			1.3	16.2	8	315	5	3
			1.8	2.3	19	27	5	0
Barrow RI	5	117	1	0	4	170	3	83
			1	0	5	262	3	72
			1.9	9.1	10	16	3	299
			2.2	6.4	10	25	18	93
Barrow HP	6	22	1	9.1	10	16	3	299
			1.1	5.9	13	5	5	293
			1.6	3.3	9	0	4	297
			2.1	0	4	170	3	83
Barrow HS	3	355	0.6	6.2	6	320	6	317
			2	5.4	8	327	6	315
			2.1	8	7	301	5	317
Morecambe	1	7	0.6	3	17	24	15	339
			1.6	3.7	14	297	16	315
			2	2.9	12	20	14	344
			2	0.9	11	119	11	69
Fleetwood	1	234	0.3	0.9	8	103	14	67
			0.9	1	13	77	14	73
			1	1.5	22	35	17	59
			2.3	9.6	6	290	6	308

Table 4a: Spatial variability of computed M_2 tidal elevations h_c (cm) and phase g_c (degrees) with distance Δ (km) between nearest nodal points and observational points from calcs 1M, 2M and 3M. Also given is the local water depth h(m).

Port	Observed				Calc 1M		Calc 2M		Calc 3M	
	h0	g0	Δ	h(m)	hc	gc	hc	gc	hc	gc
Hilbre	292	317	0.5	14.2	308	311	271	313	323	313
			1.2	5	307	311	271	314	323	313
			1.3	8.5	308	310	271	313	322	313
			1.6	16.5	310	309	271	313	322	313
Barrow RI	306	329	0.9	5	301	329	272	334	324	331
			1	5.2	301	329	272	334	324	330
			1.3	5.3	301	329	272	334	324	330
			1.6	5	303	329	273	334	324	331
Barrow HP	292	327	1.3	5.3	301	329	272	334	324	330
			1.6	7.2	301	327	271	332	323	329
			1.8	5	303	329	273	334	324	331
			2	5.2	301	330	272	334	324	330
Barrow HS	297	325	1	7.3	300	314	266	323	314	322
			1.7	5.2	300	320	269	327	318	325
			1.9	5	296	319	264	325	313	324
Morecambe	308	326	1.6	5	307	334	283	341	334	337
			1.7	5	307	338	283	342	336	338
			1.9	5	311	331	283	338	335	334
			2.5	5	307	339	284	342	336	337
Fleetwood	305	326	0.3	5	311	322	278	326	332	323
			0.7	5	310	323	278	325	330	322
			0.8	5	310	323	279	326	332	323
			1.3	5	309	321	279	326	332	323

Table 4b: Spatial variability of computed M_4 tidal elevations h_c (cm) and phase g_c (degrees) with distance Δ (km) between nearest nodal points and observational points from calcs 1M, 2M and 3M. Also given is the local water depth h(m).

Port	Observed				Calc 1M		Calc 2M		Calc 3M	
	h0	g0	Δ	h(m)	hc	gc	hc	gc		
Hilbre	20	203	0.5	14.2	31	179	23	172	30	164
			1.2	5	31	181	23	173	30	164
			1.3	8.5	29	175	22	172	30	163
			1.6	16.5	26	172	22	172	30	163
Barrow RI	30	274	0.9	5	44	241	34	253	44	235
			1	5.2	45	242	32	251	41	232
			1.3	5.3	44	240	32	251	40	232
			1.6	5	45	241	34	252	45	235
Barrow HP	26	216	1.3	5.3	44	240	31	251	40	232
			1.6	7.2	39	241	29	251	38	230
			1.8	5	45	241	34	252	45	235
			2	5.2	45	242	32	251	41	232
Barrow HS	16	200	1	7.3	15	213	15	224	23	212
			1.7	5.2	26	221	21	237	30	221
			1.9	5	22	228	17	232	25	217
Morecambe	11	217	1.6	5	66	250	61	263	83	245
			1.7	5	82	255	64	264	87	246
			1.9	5	57	244	52	260	71	240
			2.5	5	86	257	64	264	86	246
Fleetwood	11	248	0.3	5	36	220	25	227	35	205
			0.7	5	36	229	23	227	34	206
			0.8	5	36	225	25	226	36	206
			1.3	5	32	222	25	226	36	206

Table 4c: Spatial variability of computed M_6 tidal elevations h_c (cm) and phase g_c (degrees) with distance Δ (km) between nearest nodal points and observational points from calcs 1M, 2M and 3M. Also given is the local water depth h(m).

Port	Observed				Calc 1M		Calc 2M		Calc 3M	
	h0	g0	Δ	h(m)	hc	gc	hc	gc		
Hilbre	2	33	0.5	14.2	9	3	8	18	6	21
			1.2	5	8	6	8	18	6	20
			1.3	8.5	8	354	8	15	6	18
			1.6	16.5	6	349	8	15	6	17
Barrow RI	5	117	0.9	5	8	245	7	276	15	221
			1	5.2	7	250	7	283	13	223
			1.3	5.3	7	250	7	281	13	222
			1.6	5	8	239	8	274	15	219
Barrow HP	6	22	1.3	5.3	7	250	7	281	13	222
			1.6	7.2	9	243	7	275	13	220
			1.8	5	8	239	8	274	15	219
			2	5.2	7	250	7	283	13	223
Barrow HS	3	355	1	7.3	5	257	5	285	7	210
			1.7	5.2	9	265	6	280	10	215
			1.9	5	7	255	5	284	8	214
Morecambe	1	7	1.6	5	15	207	13	229	26	198
			1.7	5	21	183	13	222	27	194
			1.9	5	15	226	13	243	24	208
			2.5	5	23	181	13	223	27	196
Fleetwood	1	234	0.3	5	9	258	7	278	10	218
			0.7	5	10	244	7	278	10	216
			0.8	5	10	252	7	282	10	219
			1.3	5	10	249	8	280	11	218

Fig 1(a):

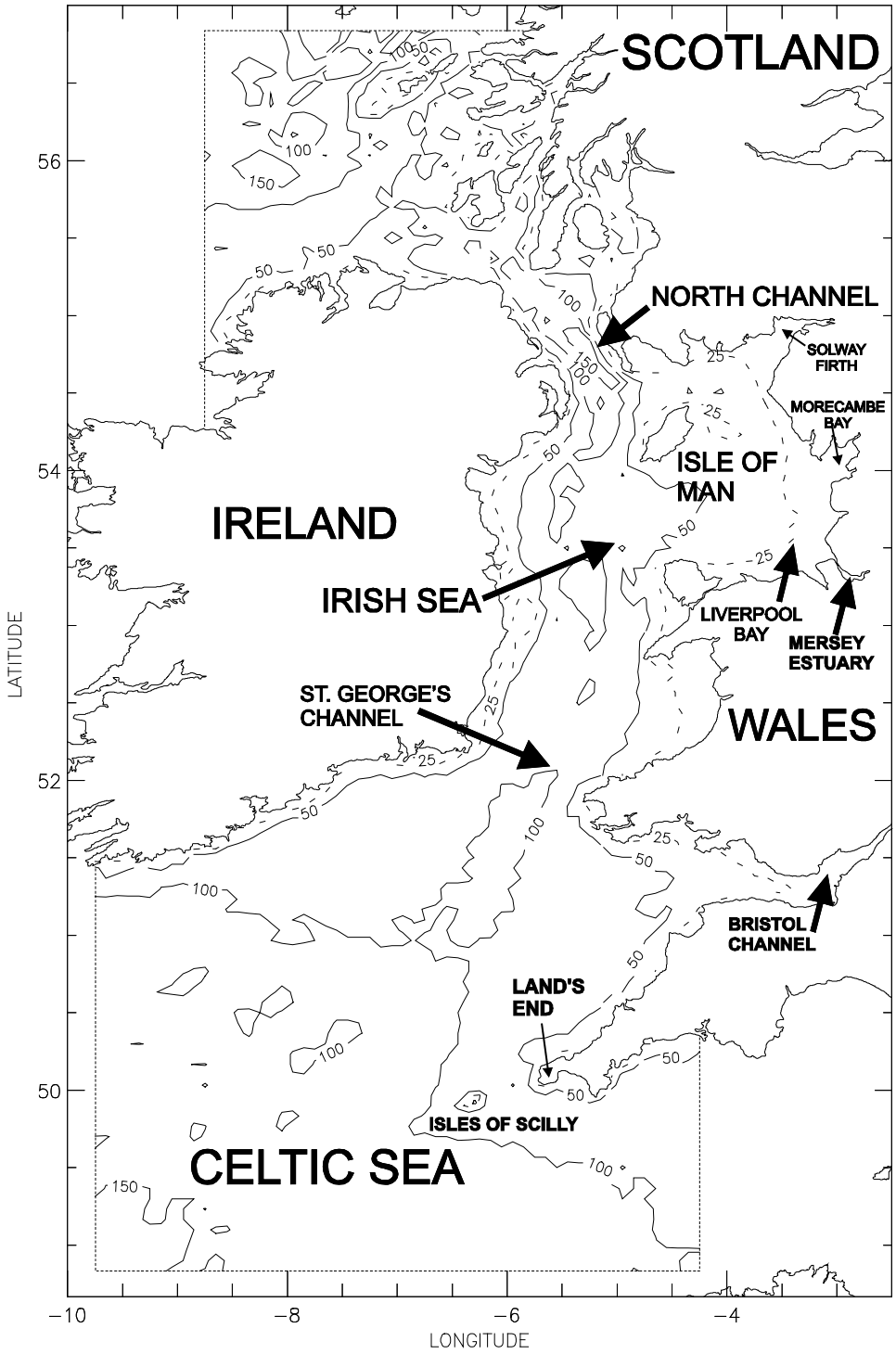
SCOTLAND
NORTH CHANNEL
SOLWAY FIRTH
MORECAMBE BAY
ISLE OF MAN
IRELAND
IRISH SEA
LIVERPOOL BAY
MERSEY ESTUARY
ST. GEORGE'S CHANNEL
WALES
BRISTOL CHANNEL
LAND'S END
ISLES OF SCILLY
CELTIC SEA
LATITUDE
LONGITUDE
56
54
52
50
−10
−8
−6
−4

Fig 1(b):

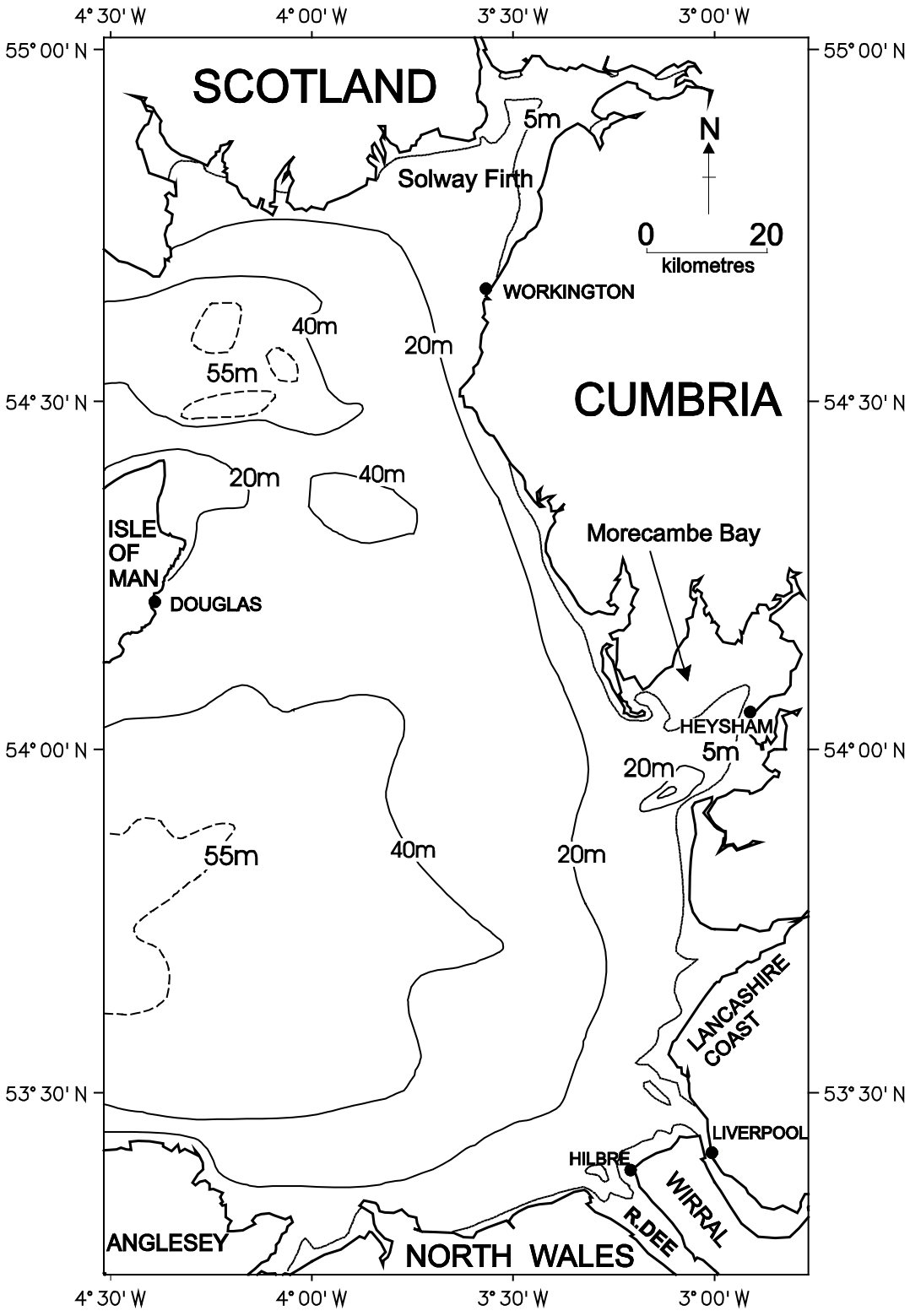
4° 30' W
4° 00' W
3° 30' W
3° 00' W
55° 00' N
54° 30' N
54° 00' N
53° 30' N
SCOTLAND
5m
N
Solway Firth
0
20
kilometres
WORKINGTON
40m
20m
55m
CUMBRIA
20m
40m
ISLE
OF
MAN
DOUGLAS
Morecambe Bay
HEYSHAM
5m
20m
55m
40m
20m
LANCASHIRE
COAST
LIVERPOOL
HILBRE
WIRRAL
R.DEE
ANGLESEY
NORTH WALES

Fig 2:

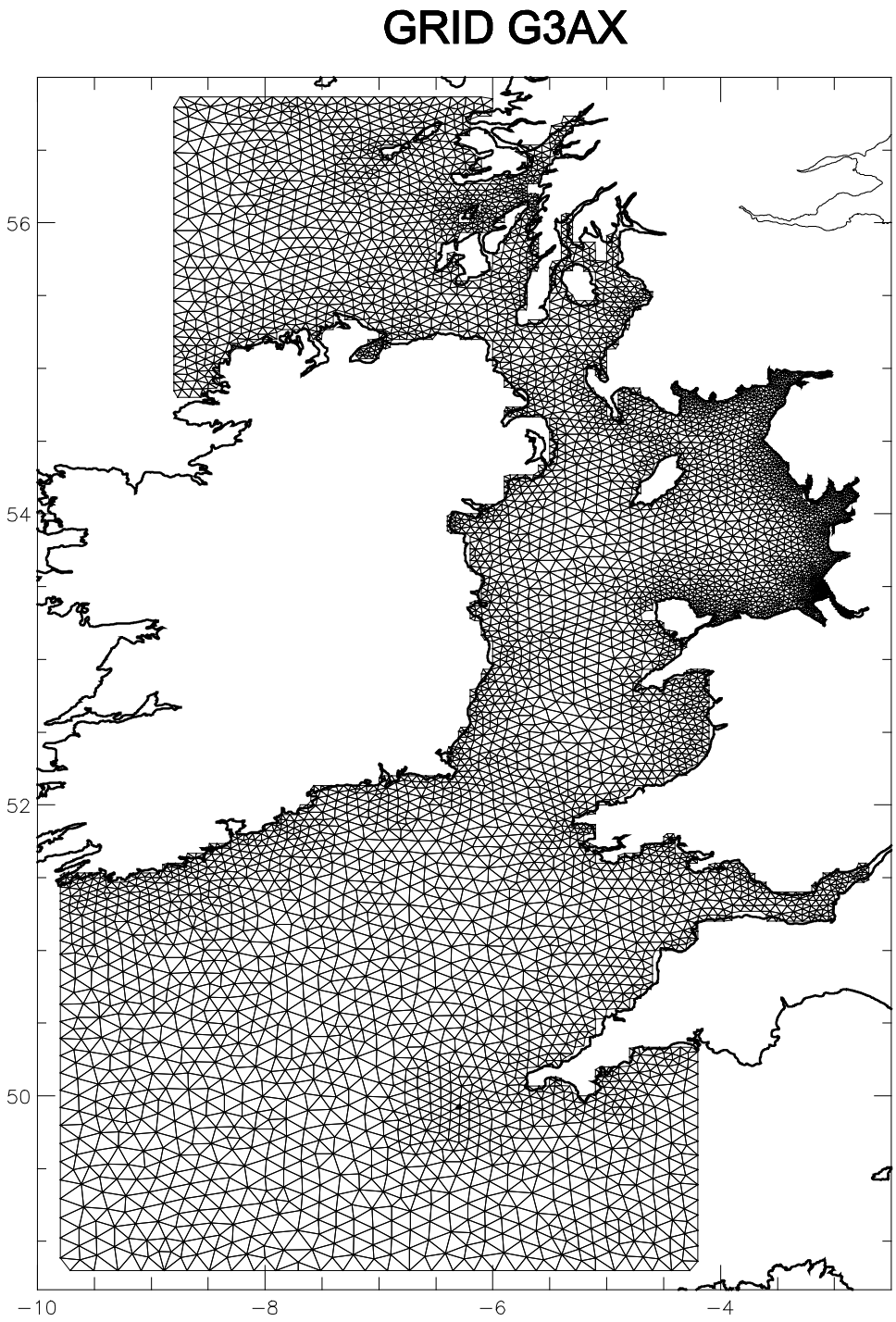

Fig 3:

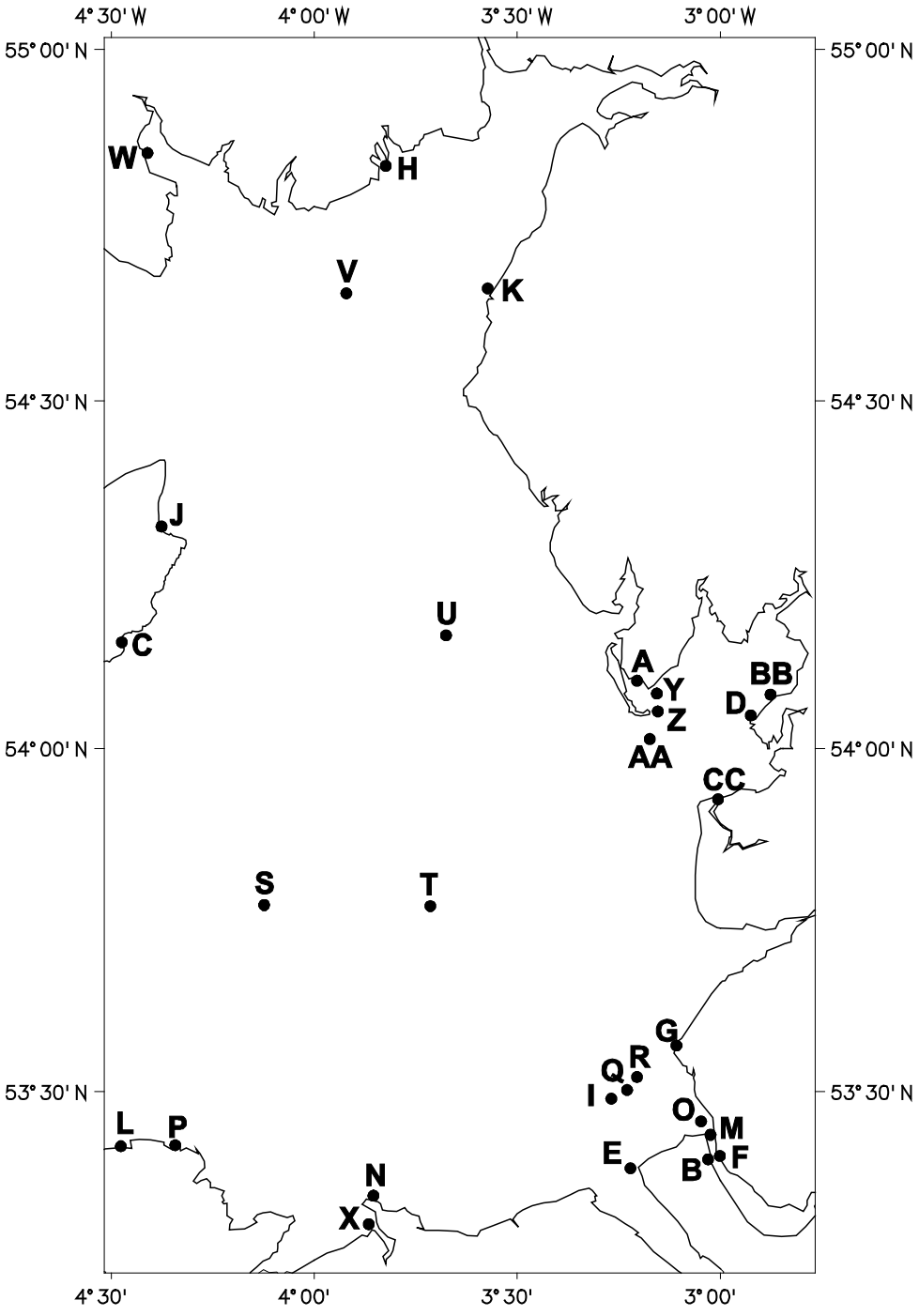
4° 30' W
4° 00' W
3° 30' W
3° 00' W
55° 00' N
54° 30' N
54° 00' N
53° 30' N
4° 30'
4° 00'
3° 30'
3° 00'
W
H
V
K
J
C
U
A
Y
Z
AA
BB
D
CC
S
T
G
Q
R
I
O
M
F
E
B
L
P
N
X

Fig 4a(i):

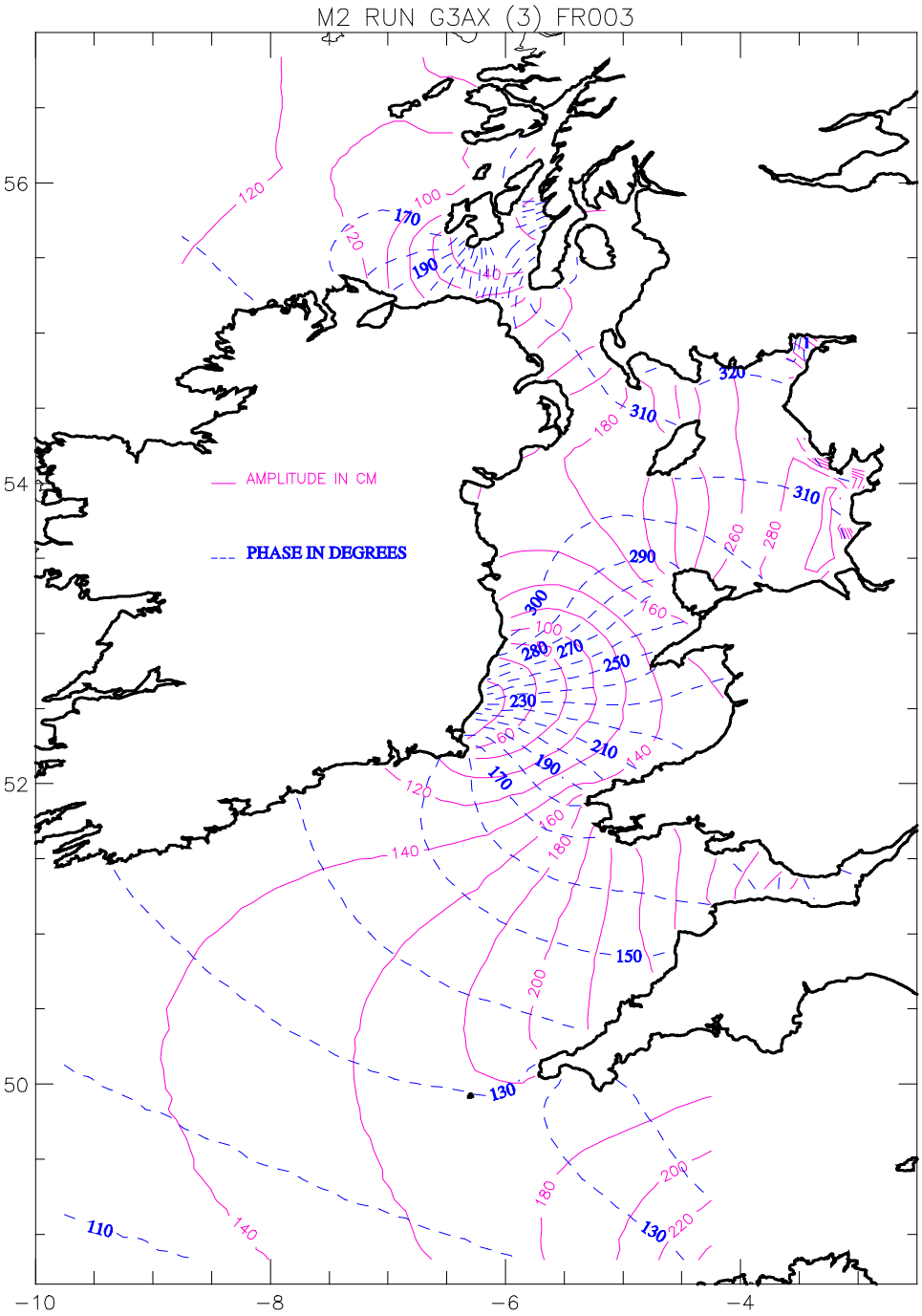
M2 RUN G3AX (3) FR003
AMPLITUDE IN CM
PHASE IN DEGREES
56
54
52
50
−10
−8
−6
−4

Fig 4a(ii):

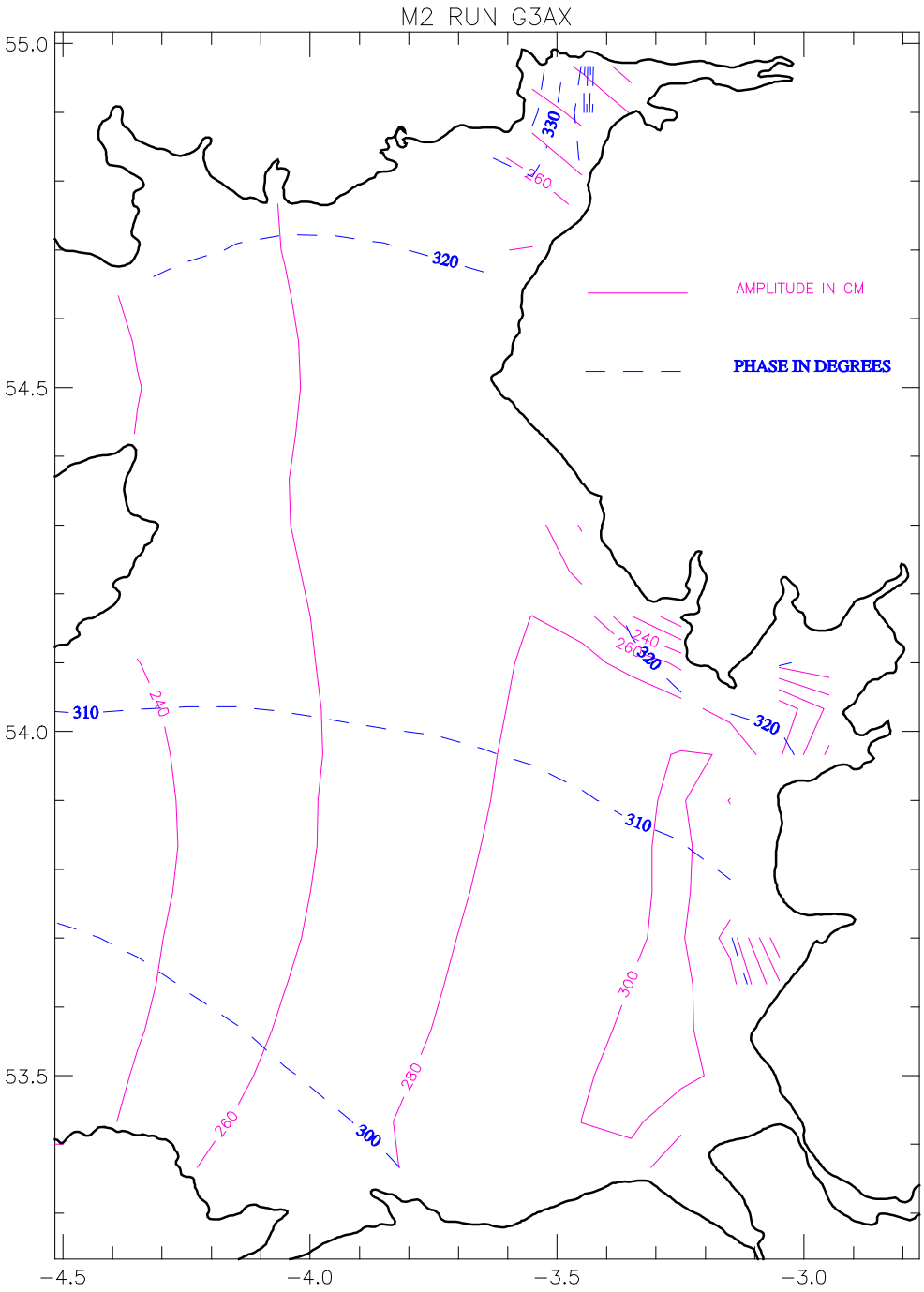
M2 RUN G3AX
55.0
54.5
54.0
53.5
−4.5
−4.0
−3.5
−3.0
AMPLITUDE IN CM
PHASE IN DEGREES
330
320
310
300
260
240
280

Fig 4b(i):

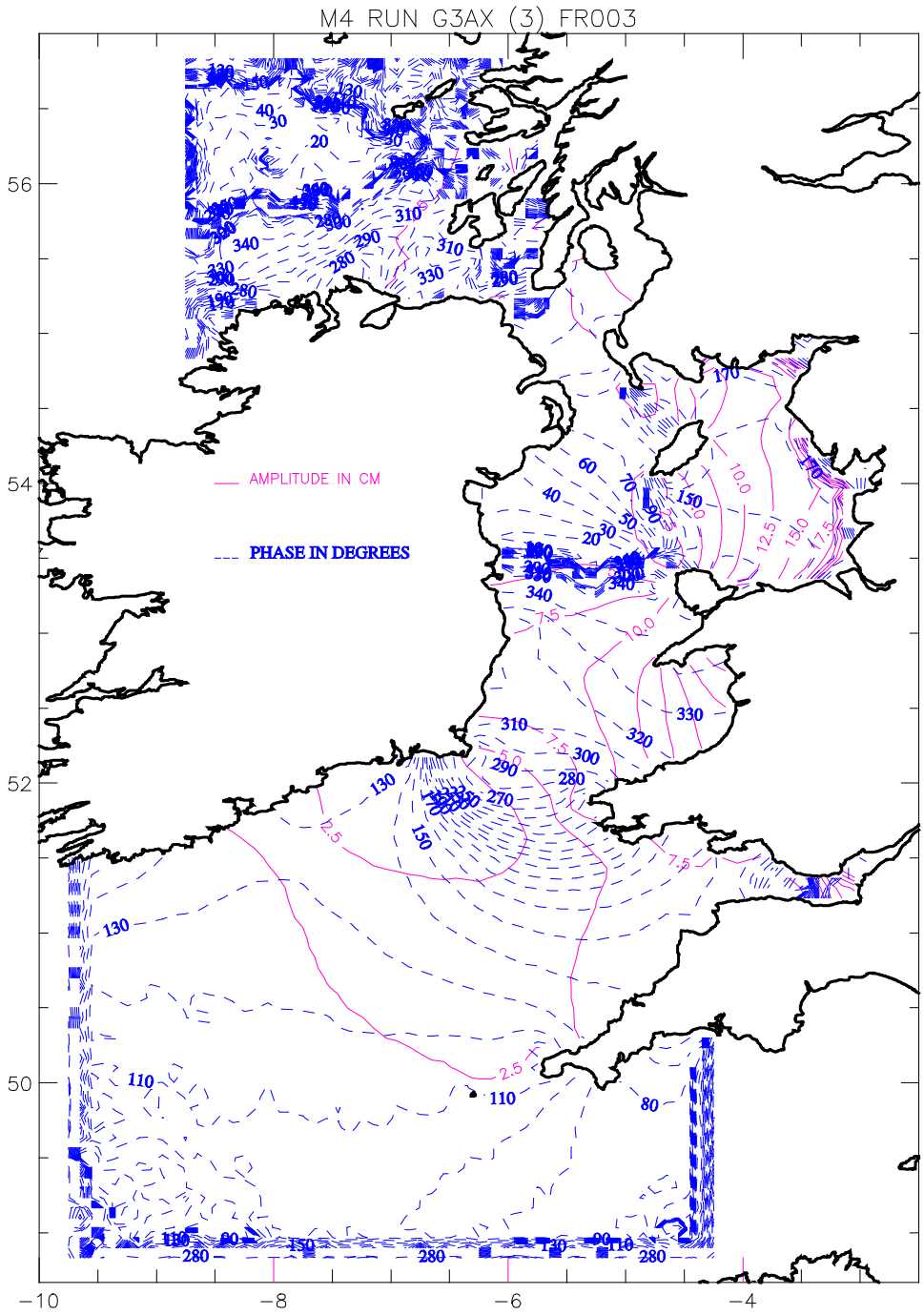
M4 RUN G3AX (3) FR003
AMPLITUDE IN CM
PHASE IN DEGREES
56
54
52
50
−10
−8
−6
−4

Fig 4b(ii):

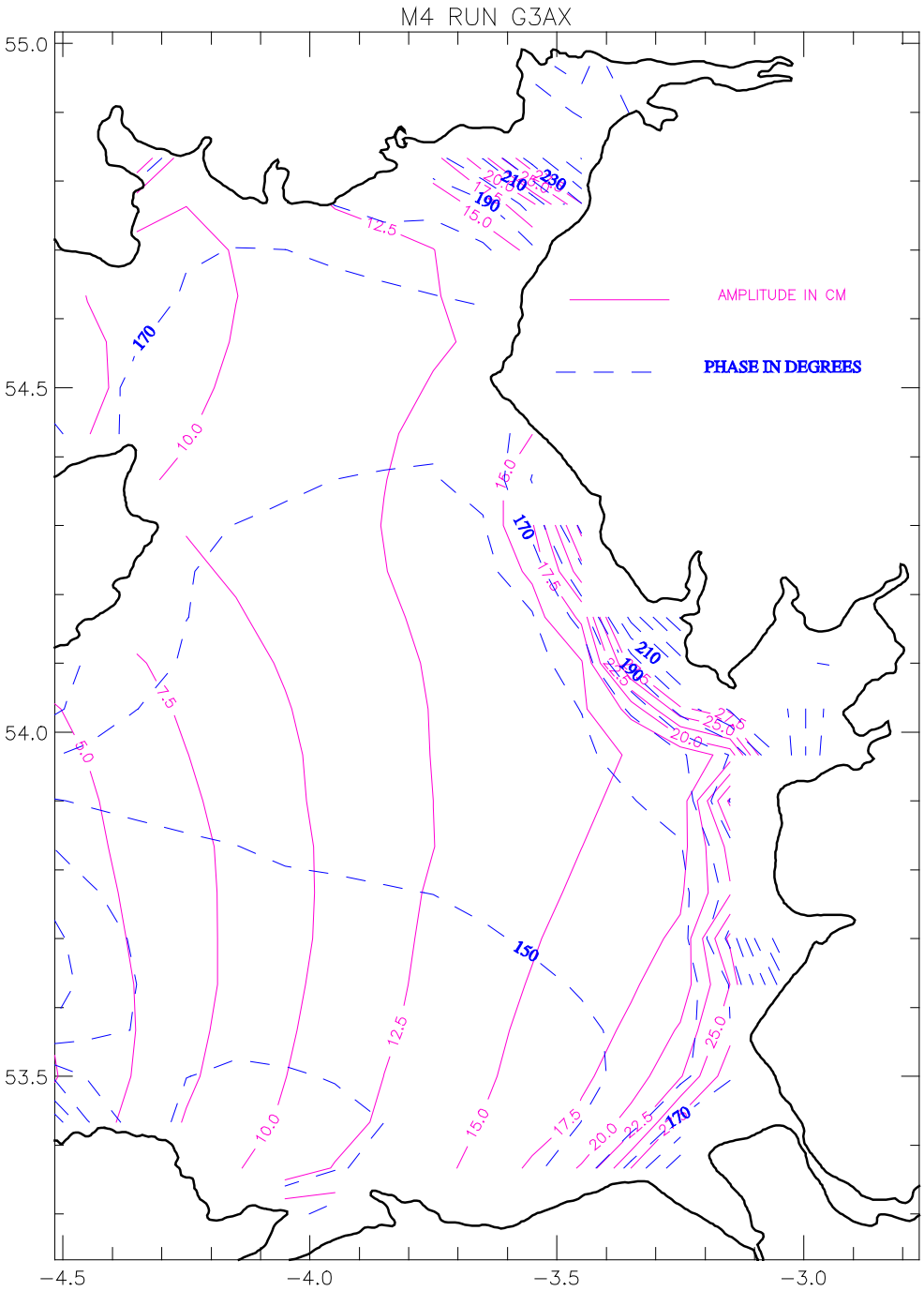
M4 RUN G3AX
55.0
54.5
54.0
53.5
−4.5
−4.0
−3.5
−3.0
AMPLITUDE IN CM
PHASE IN DEGREES

Fig 4c(i):

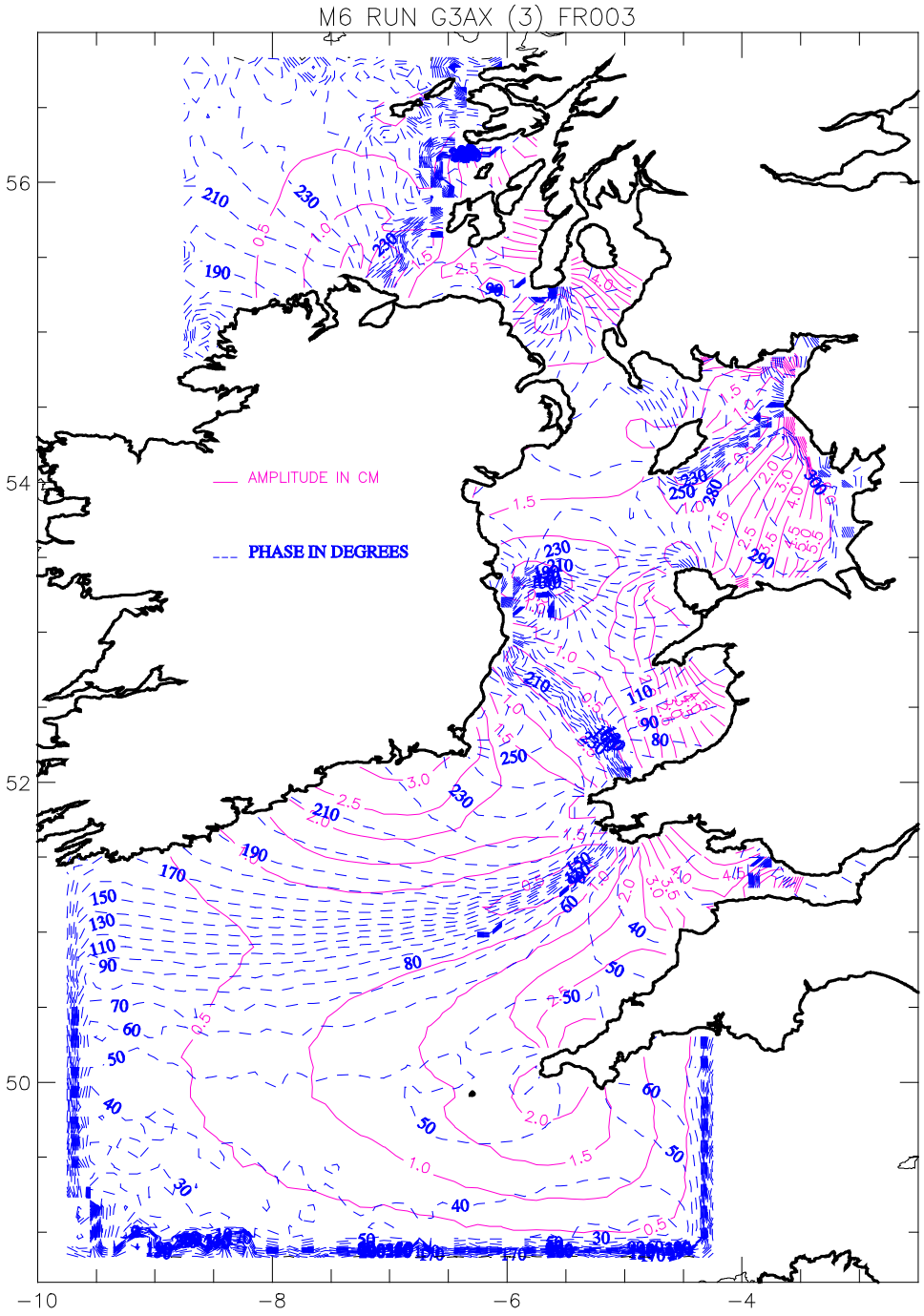
M6 RUN G3AX (3) FR003
AMPLITUDE IN CM
PHASE IN DEGREES
56
54
52
50
−10
−8
−6
−4

Fig 4c(ii):

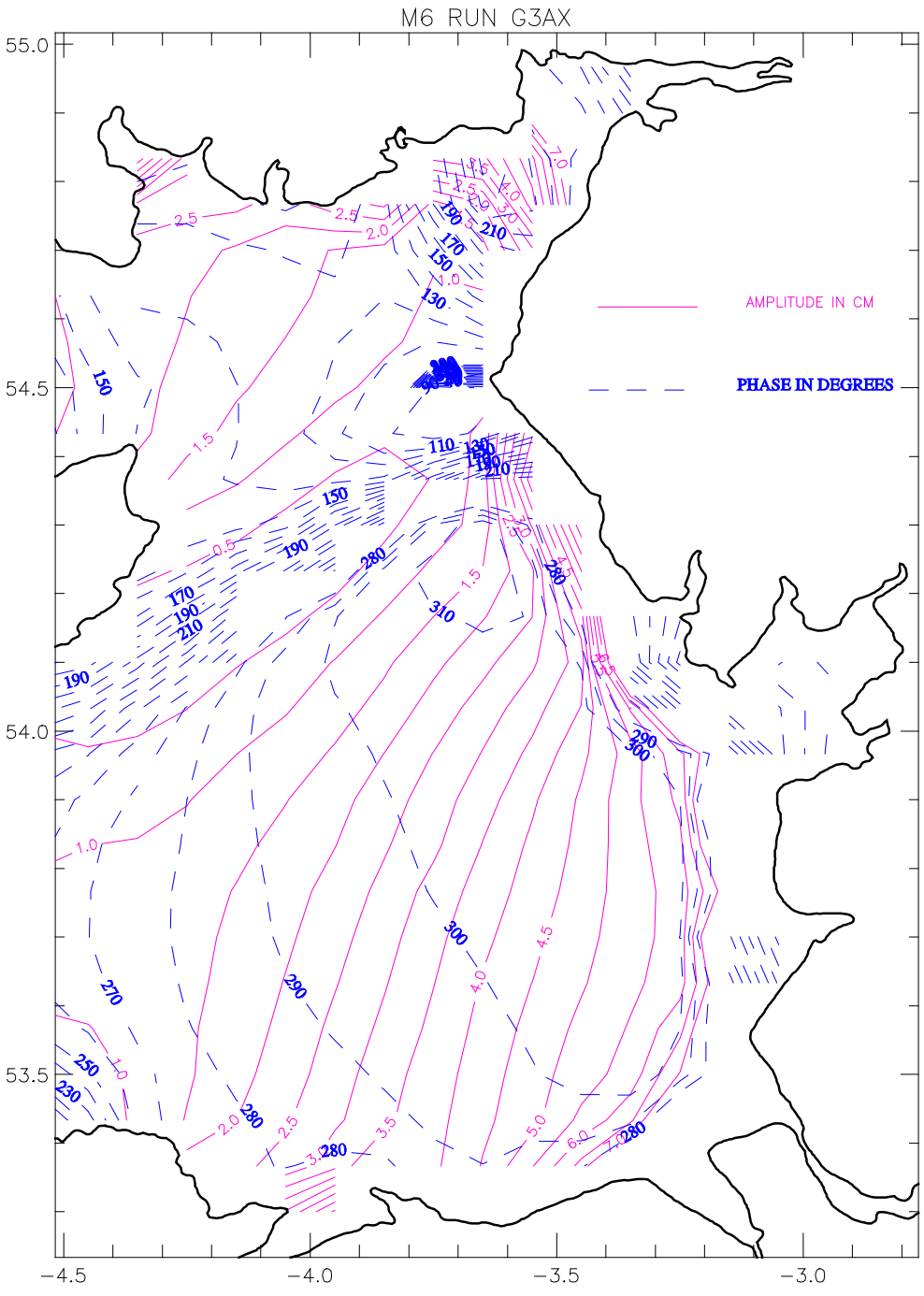
M6 RUN G3AX
55.0
54.5
54.0
53.5
−4.5
−4.0
−3.5
−3.0
AMPLITUDE IN CM
PHASE IN DEGREES

Fig 5a:

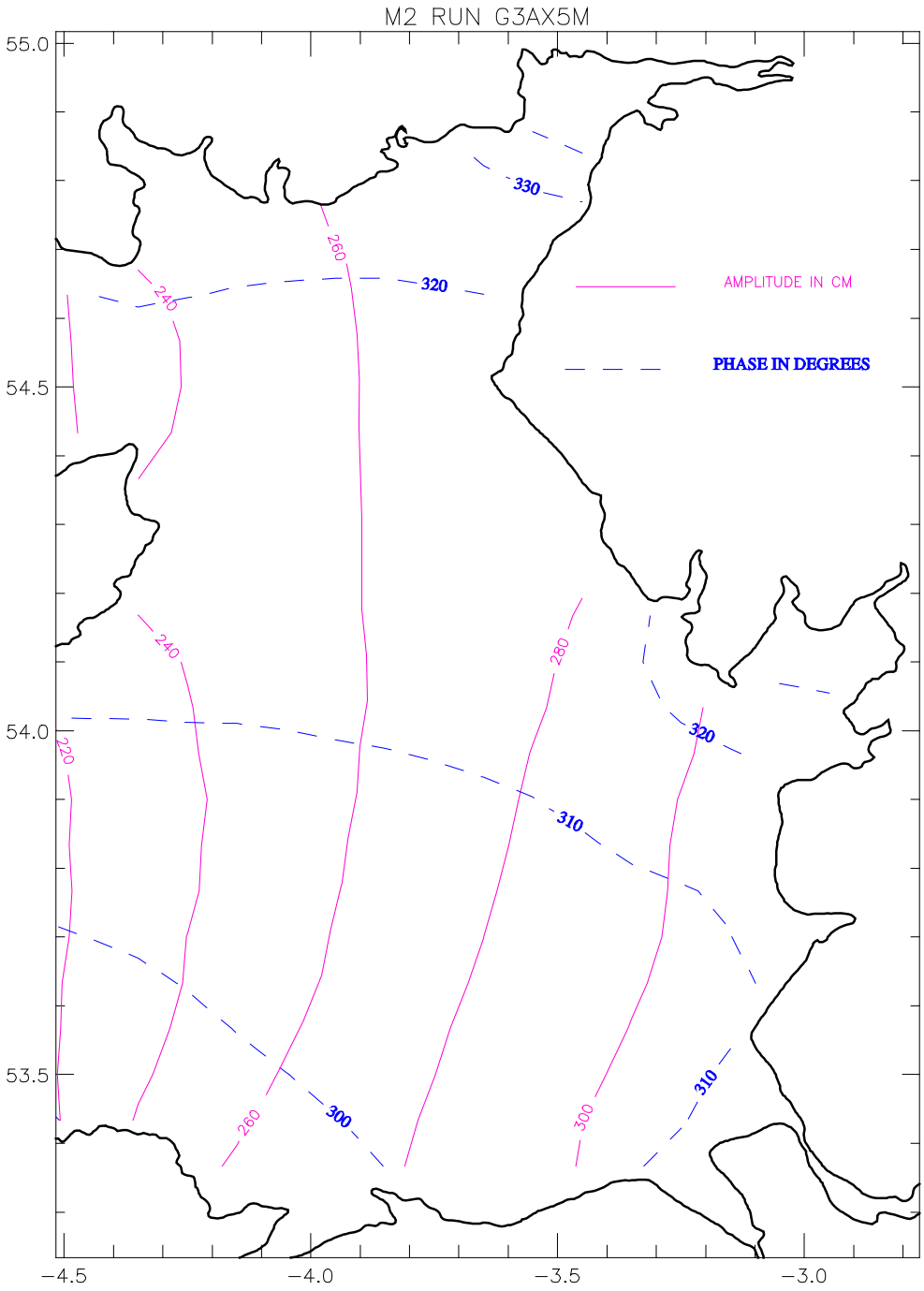
M2 RUN G3AX5M
55.0
54.5
54.0
53.5
−4.5
−4.0
−3.5
−3.0
AMPLITUDE IN CM
PHASE IN DEGREES
330
320
310
300
260
240
220
280

Fig 5b:

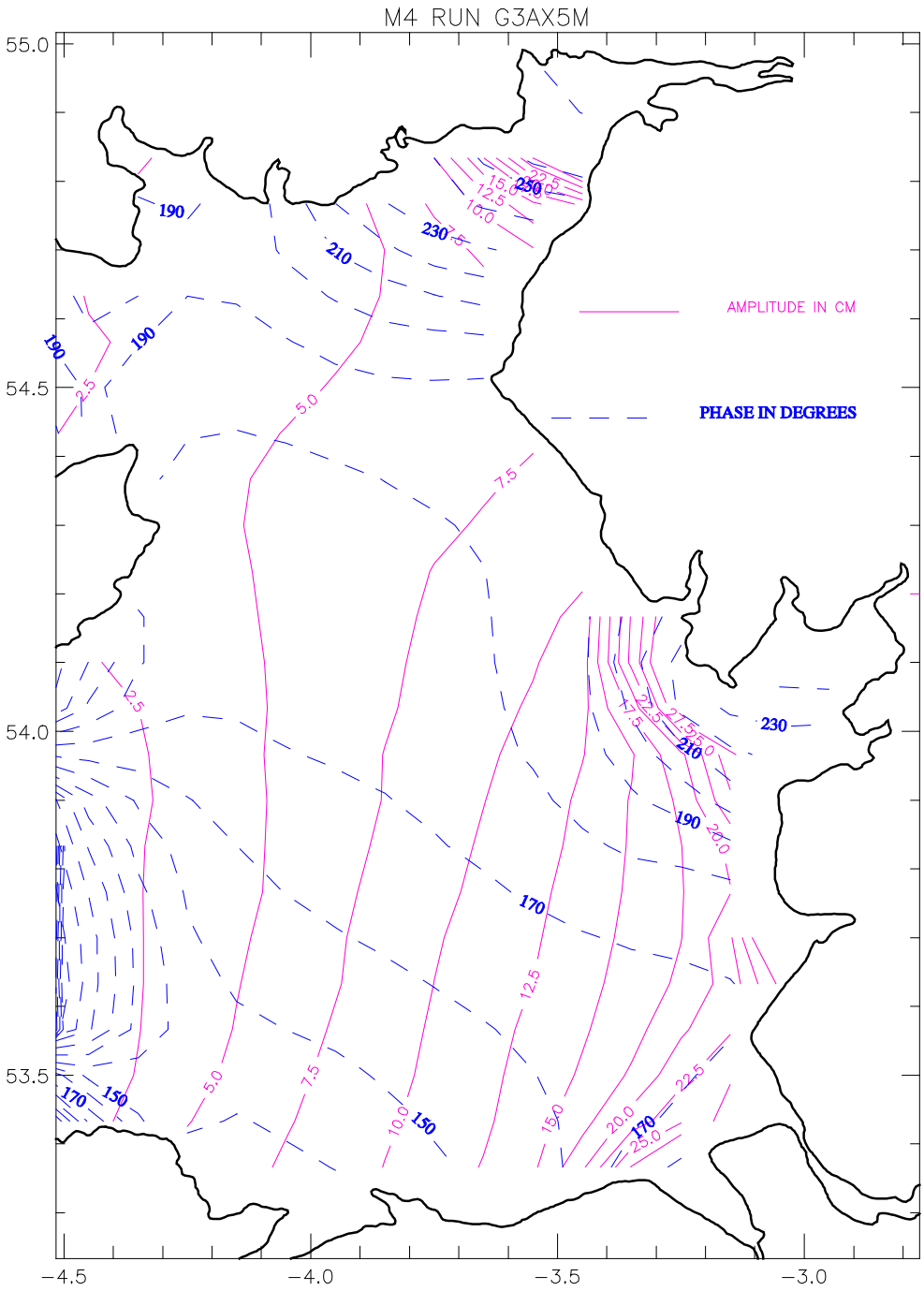
M4 RUN G3AX5M
AMPLITUDE IN CM
PHASE IN DEGREES
55.0
54.5
54.0
53.5
−4.5
−4.0
−3.5
−3.0

Fig 5c:

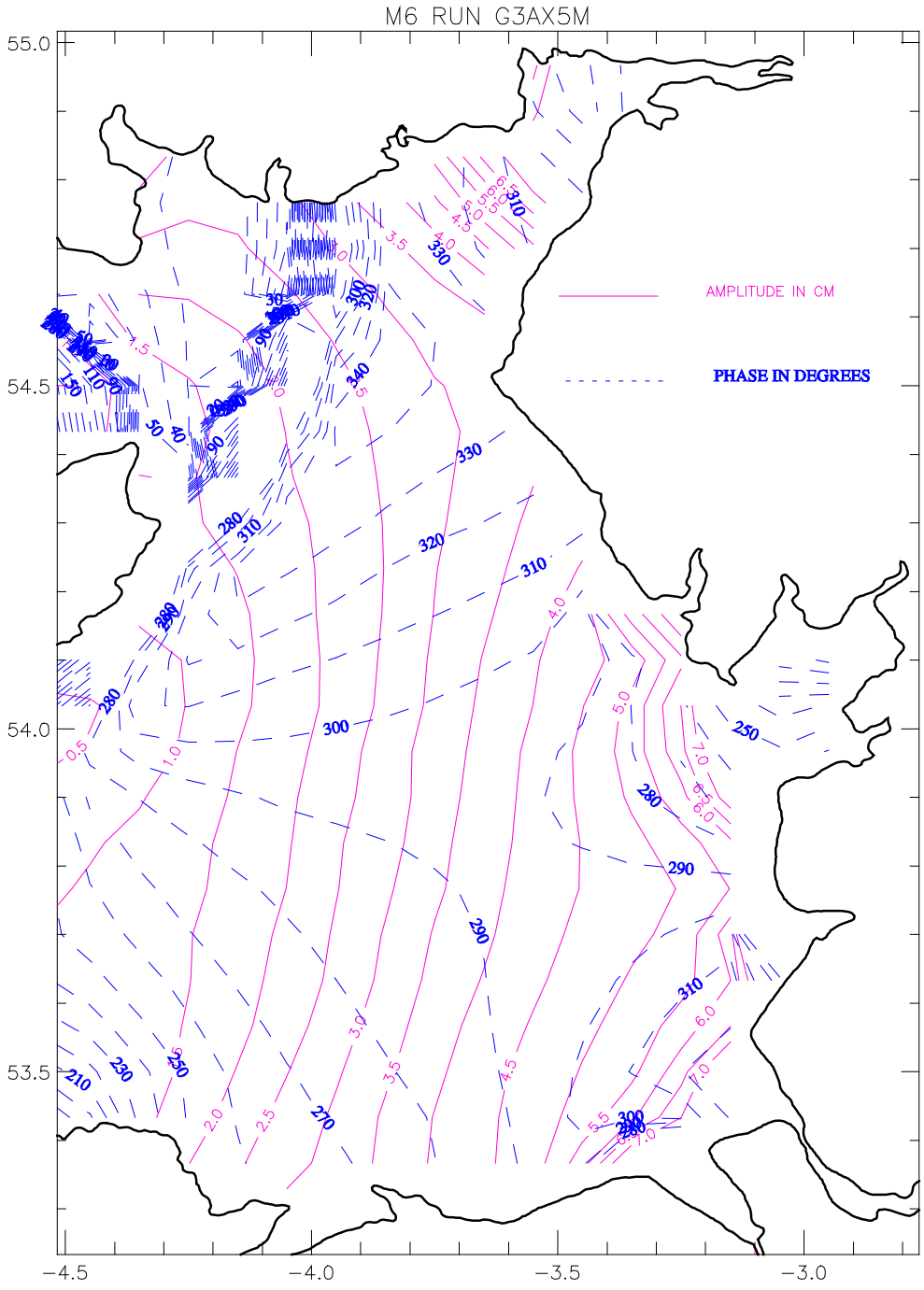
M6 RUN G3AX5M
AMPLITUDE IN CM
PHASE IN DEGREES
55.0
54.5
54.0
53.5
−4.5
−4.0
−3.5
−3.0

Fig 6a(i):

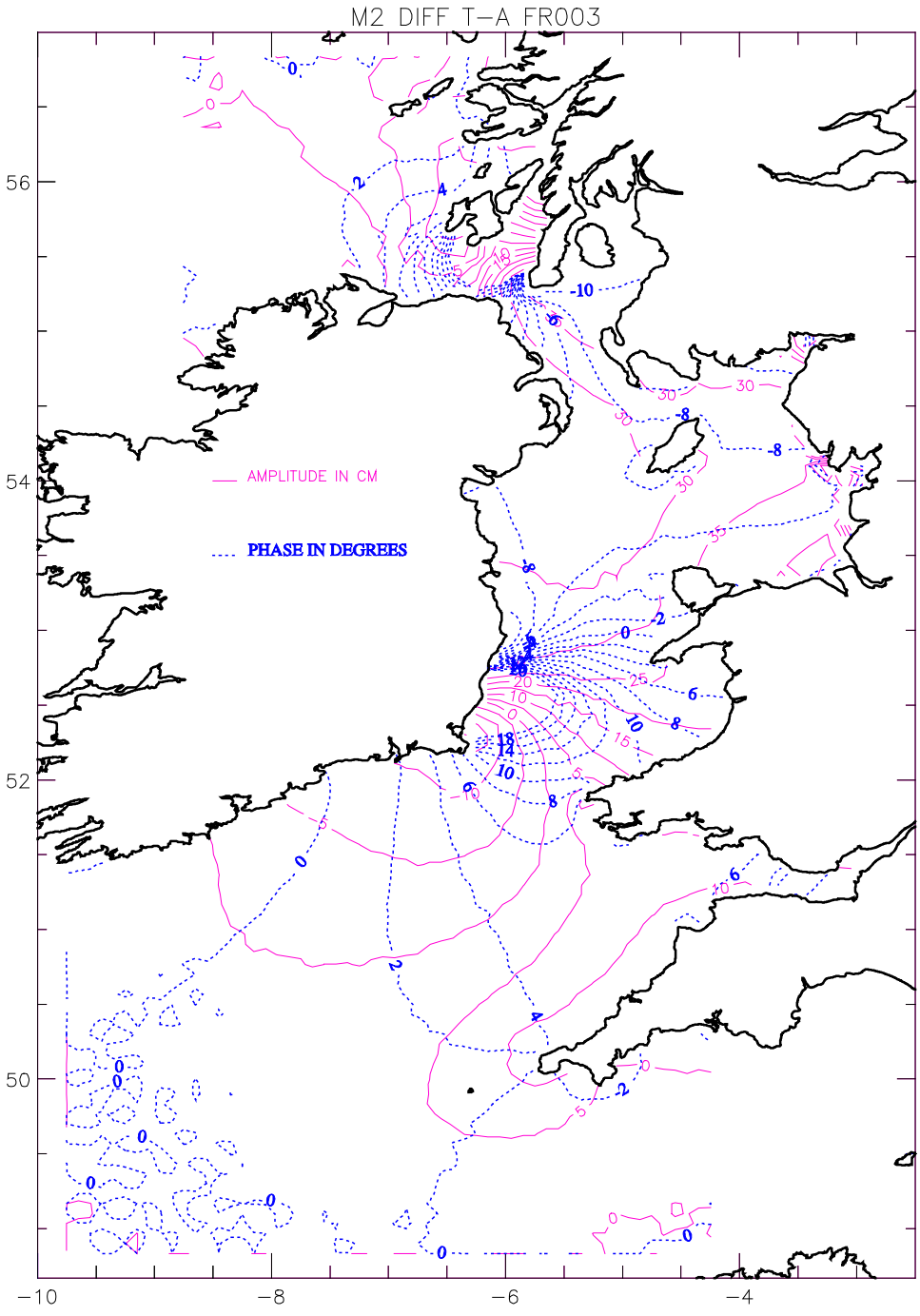
M2 DIFF T-A FR003
AMPLITUDE IN CM
PHASE IN DEGREES
56
54
52
50
-10
-8
-6
-4

Fig 6a(ii):

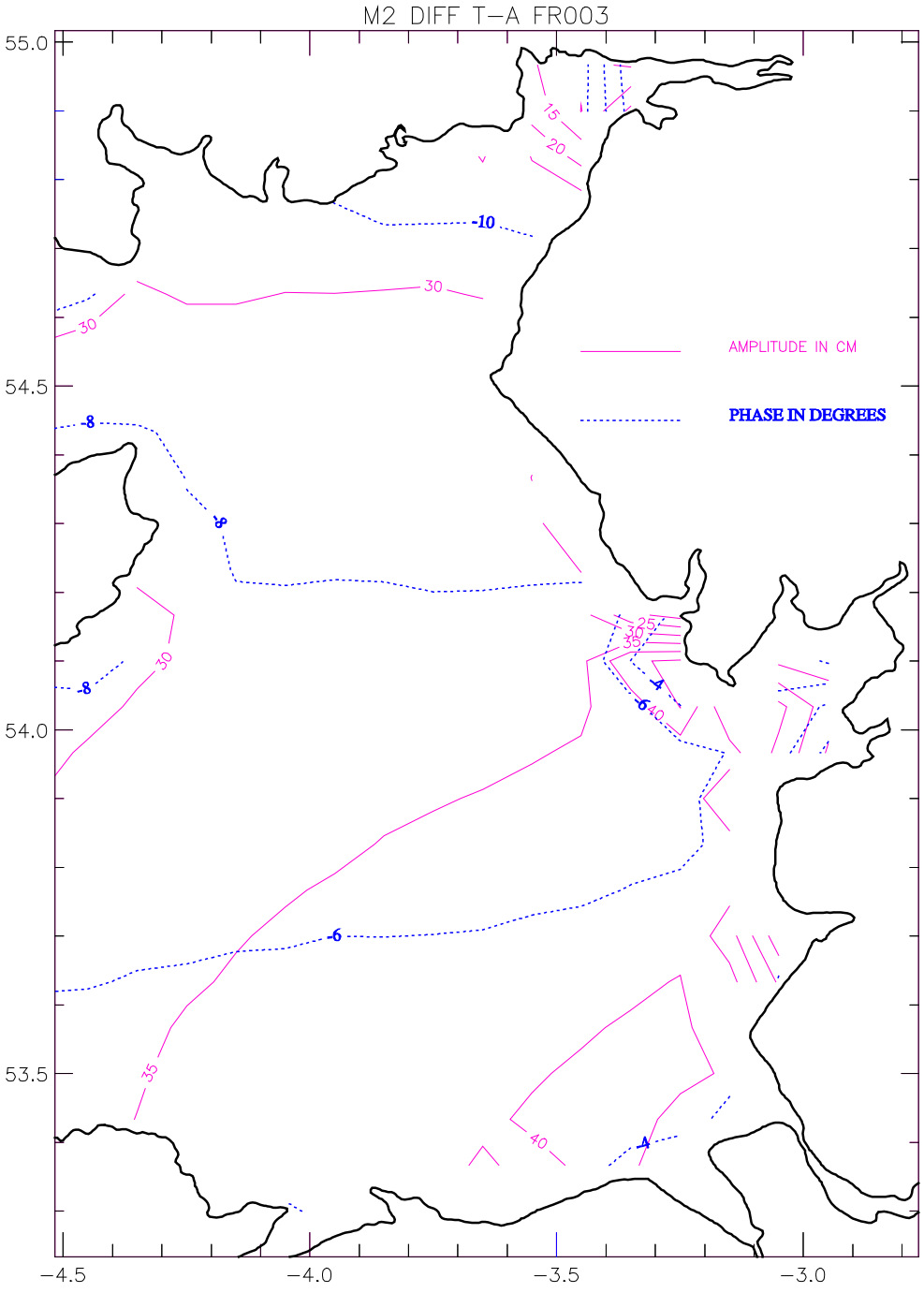
M2 DIFF T–A FR003
55.0
54.5
54.0
53.5
−4.5
−4.0
−3.5
−3.0
AMPLITUDE IN CM
PHASE IN DEGREES
15
20
-10
30
30
-8
-8
-8
30
25
30
35
-4
40
-6
35
40
-4

Fig 6b(i):

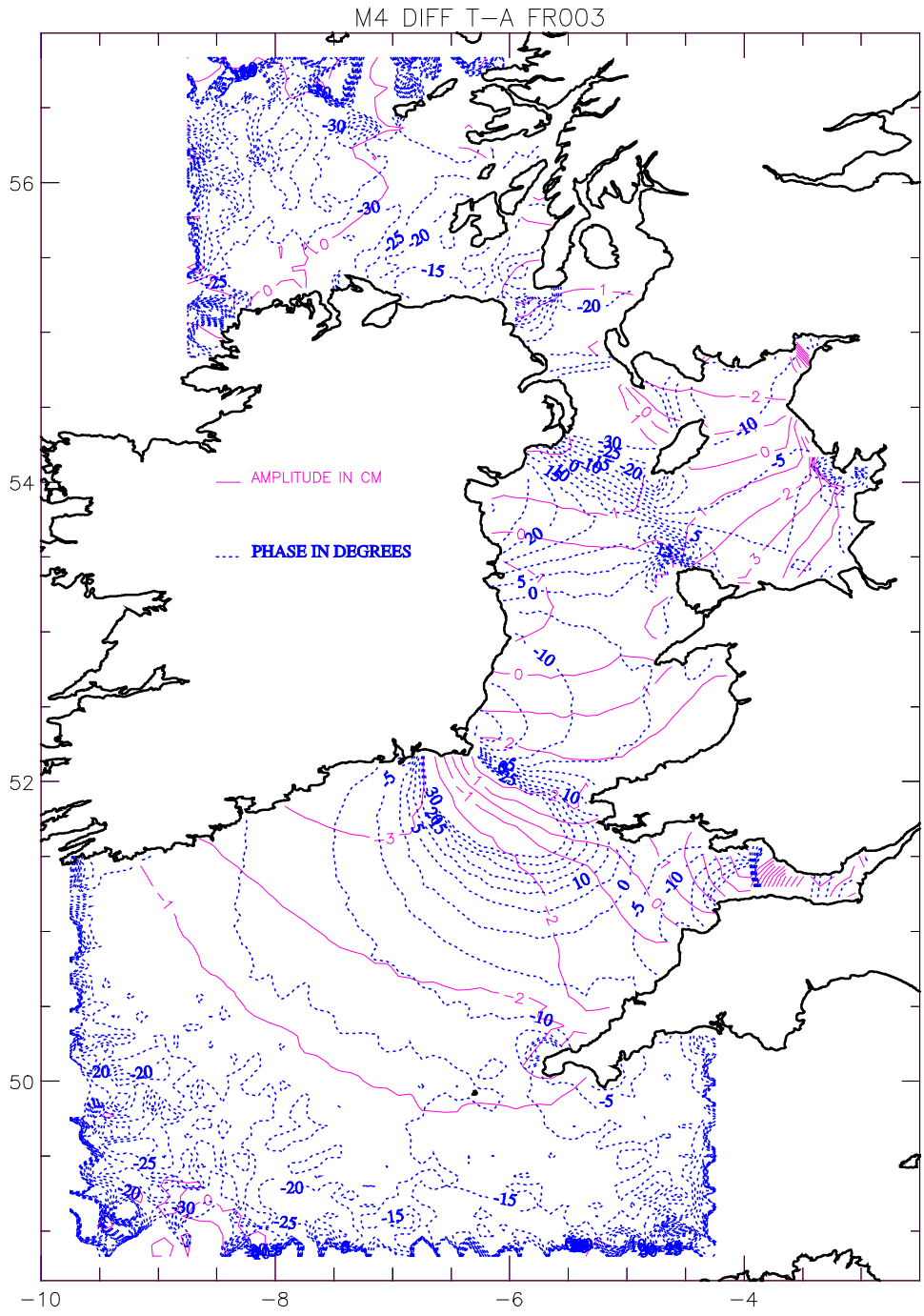
M4 DIFF T−A FR003
AMPLITUDE IN CM
PHASE IN DEGREES
56
54
52
50
−10
−8
−6
−4

Fig 6b(ii):

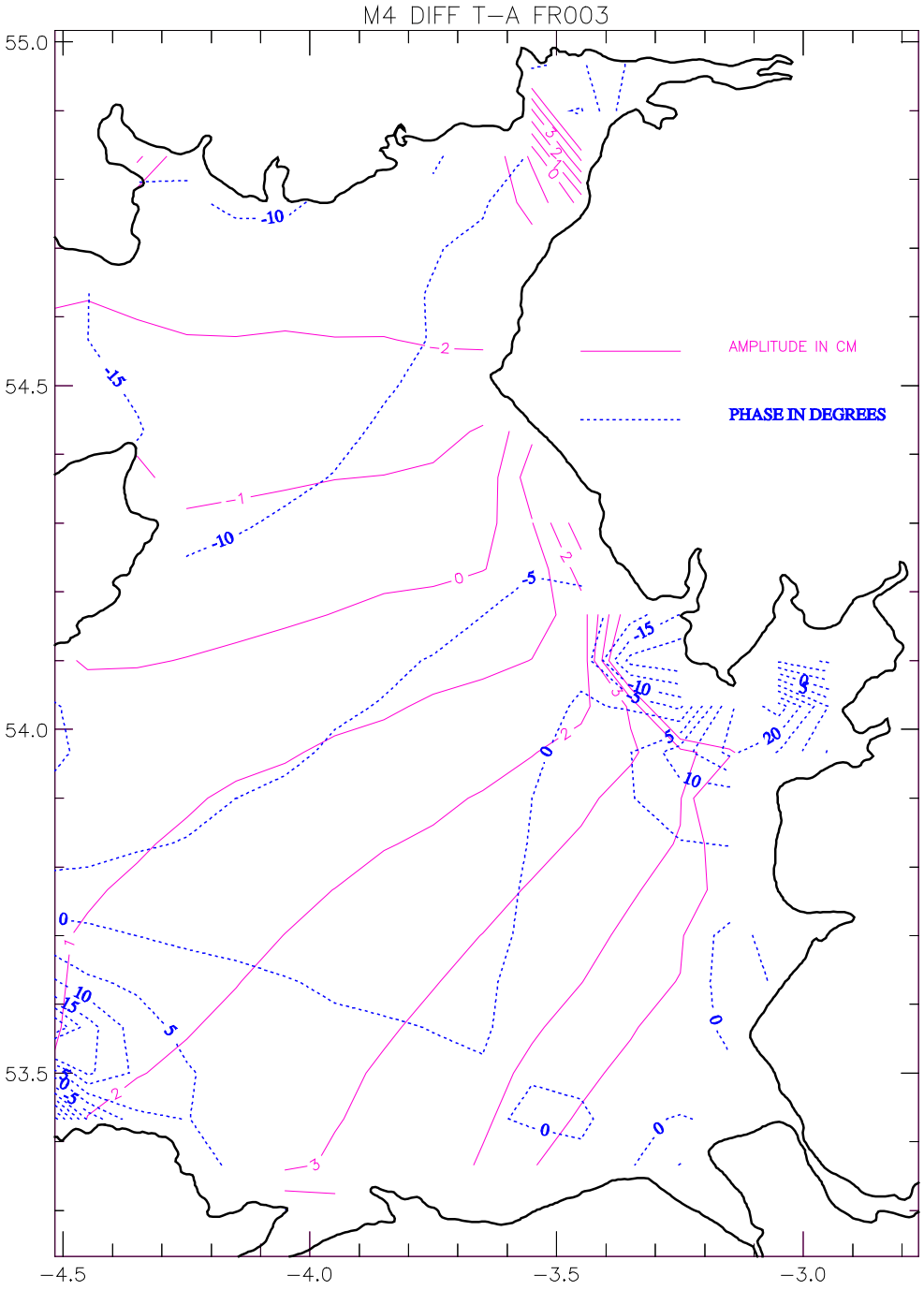
M4 DIFF T–A FR003
55.0
54.5
54.0
53.5
−4.5
−4.0
−3.5
−3.0
AMPLITUDE IN CM
PHASE IN DEGREES

Fig 6c(i):

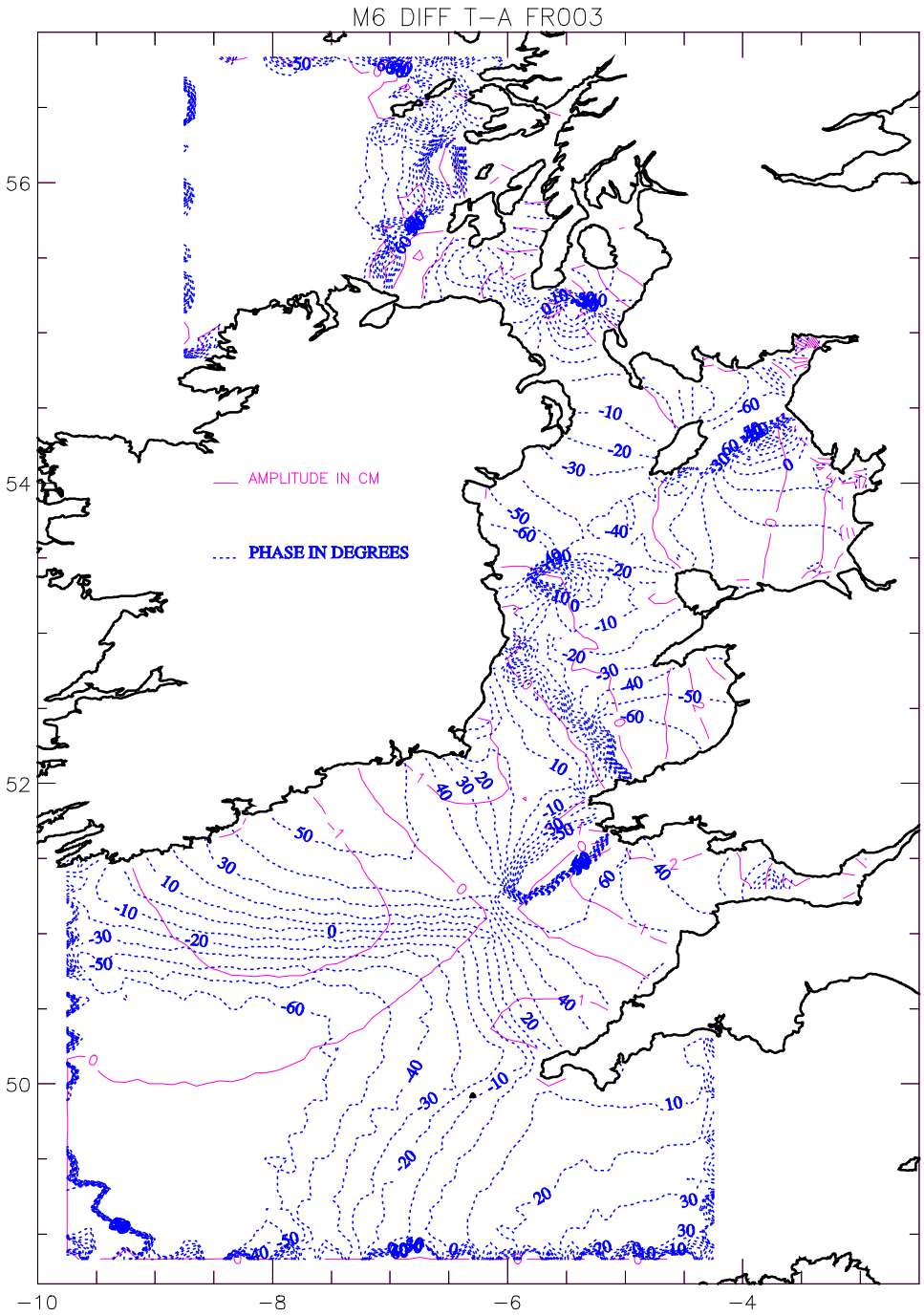
M6 DIFF T−A FR003
AMPLITUDE IN CM
PHASE IN DEGREES
56
54
52
50
−10
−8
−6
−4

Fig 6c(ii):

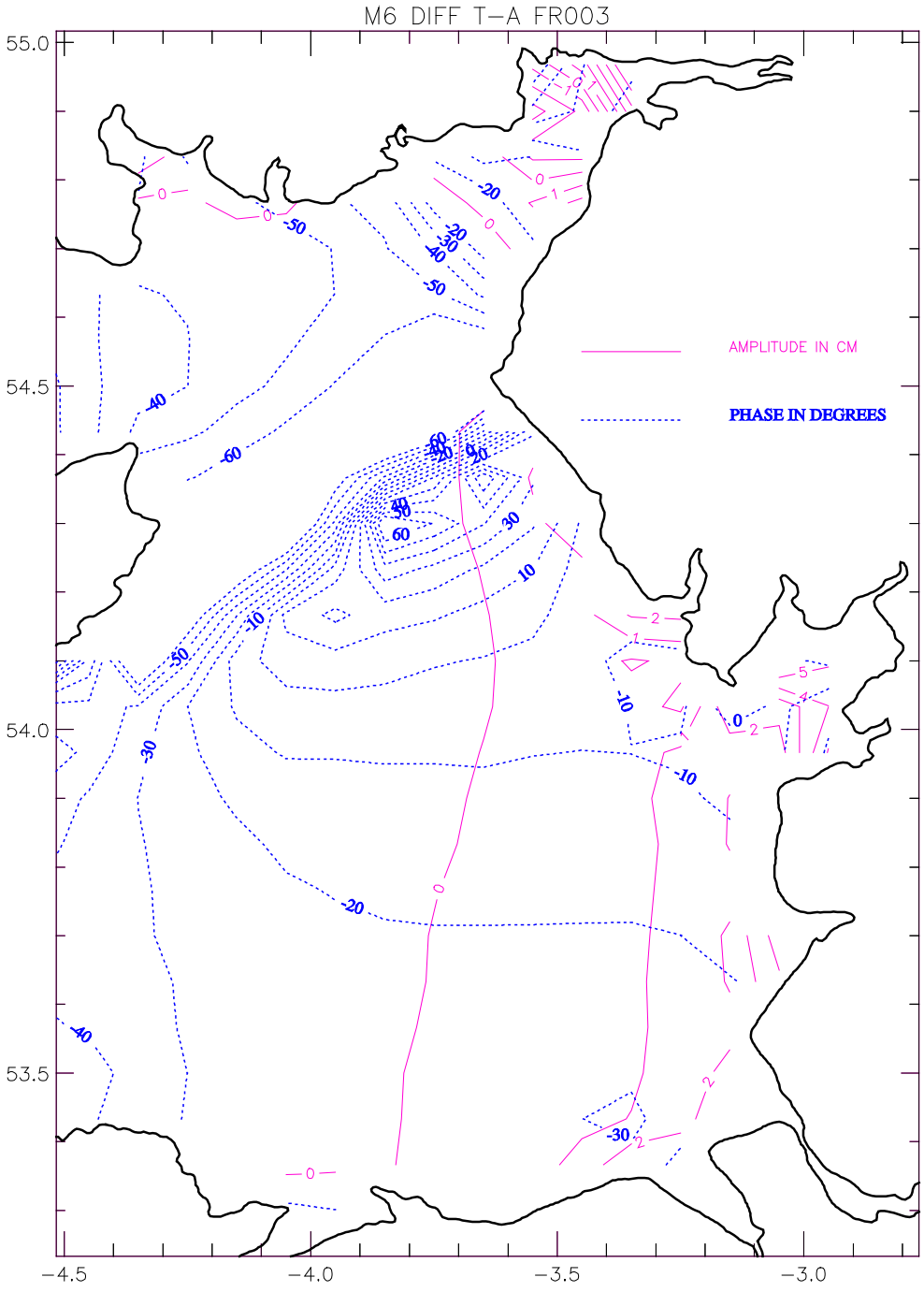
M6 DIFF T–A FR003
55.0
54.5
54.0
53.5
–4.5
–4.0
–3.5
–3.0
AMPLITUDE IN CM
PHASE IN DEGREES

Fig 7a:

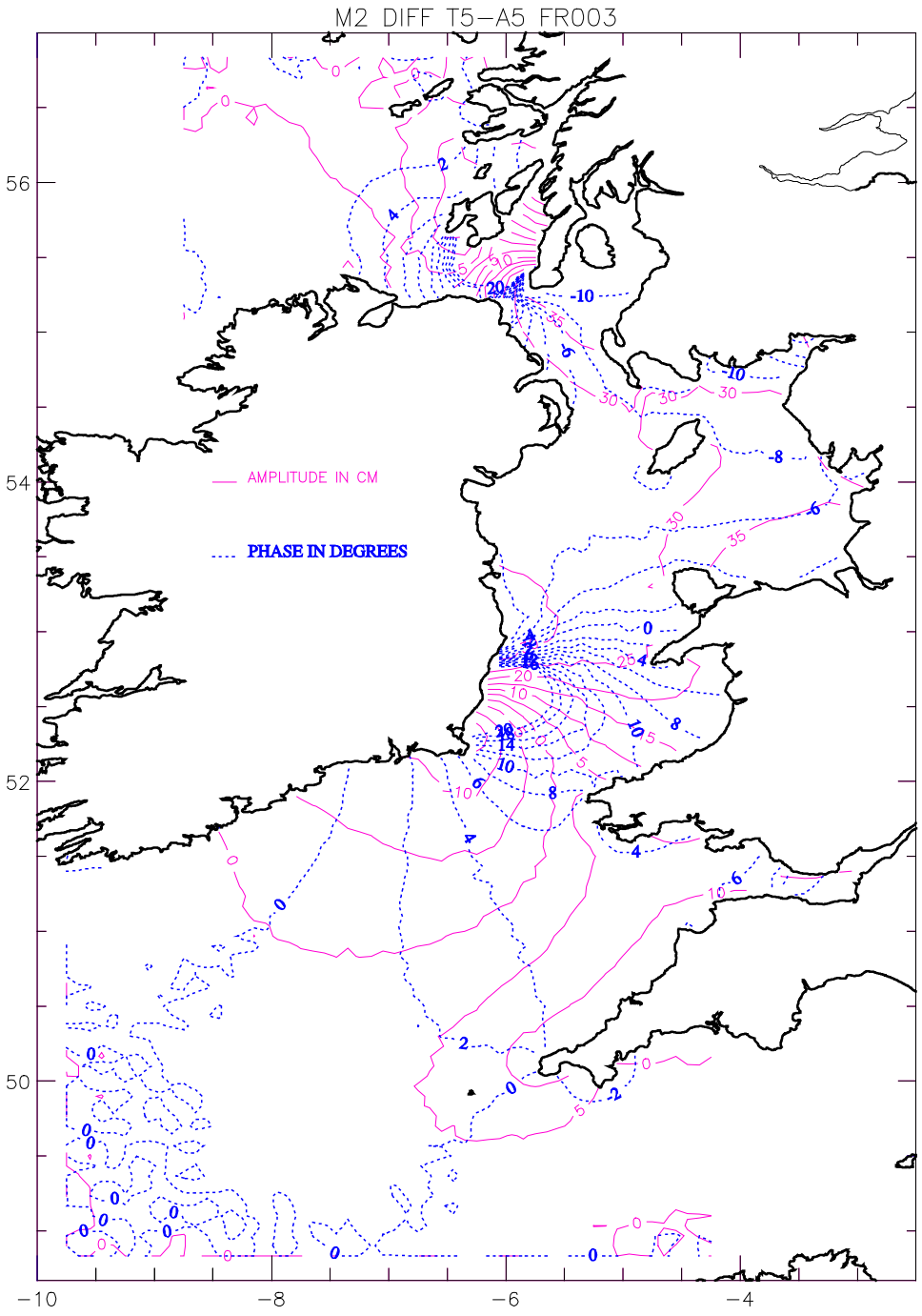
M2 DIFF T5−A5 FR003
AMPLITUDE IN CM
PHASE IN DEGREES
56
54
52
50
−10
−8
−6
−4

Fig 7b:

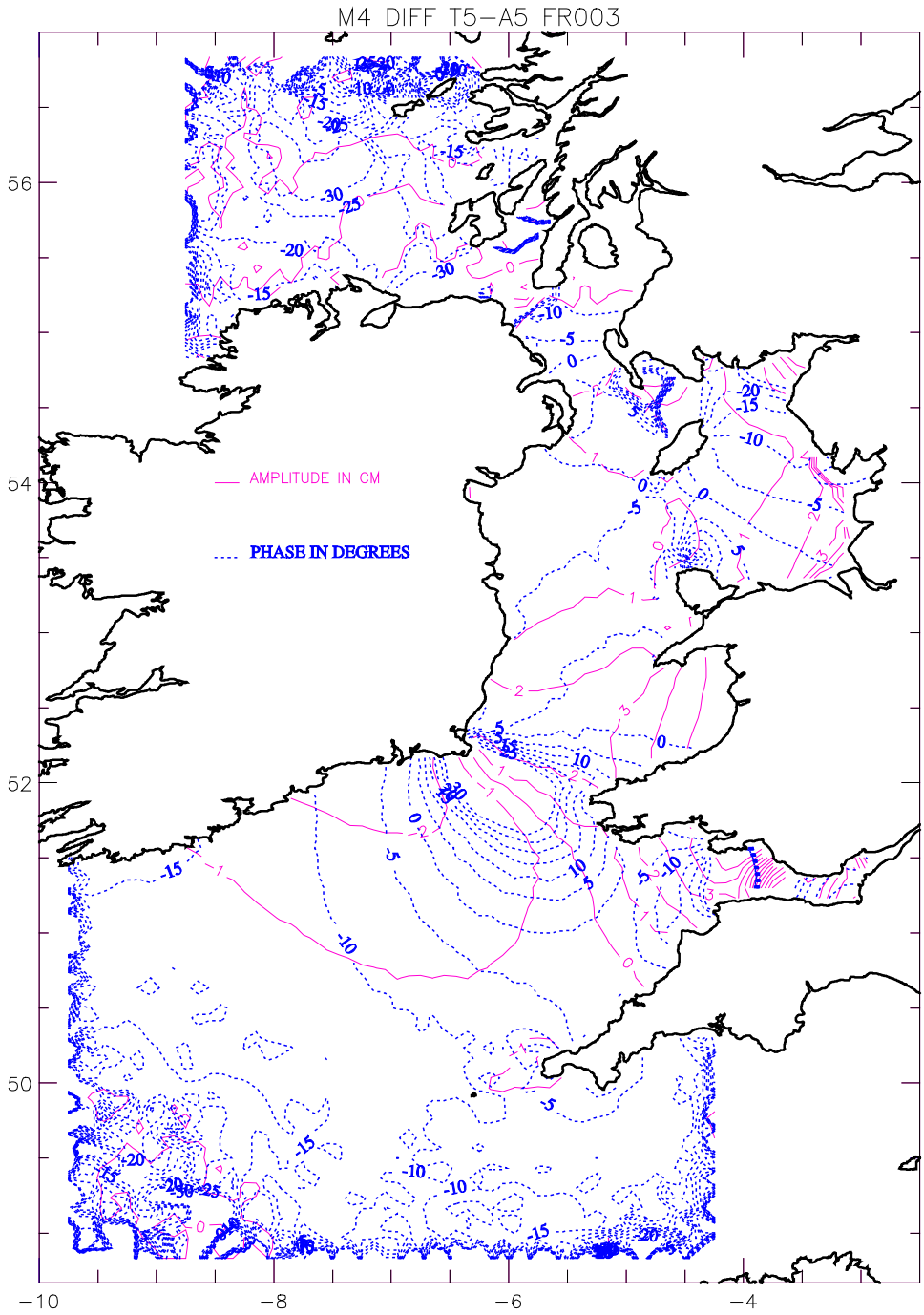
M4 DIFF T5−A5 FR003
AMPLITUDE IN CM
PHASE IN DEGREES
56
54
52
50
−10
−8
−6
−4

Fig 8a:

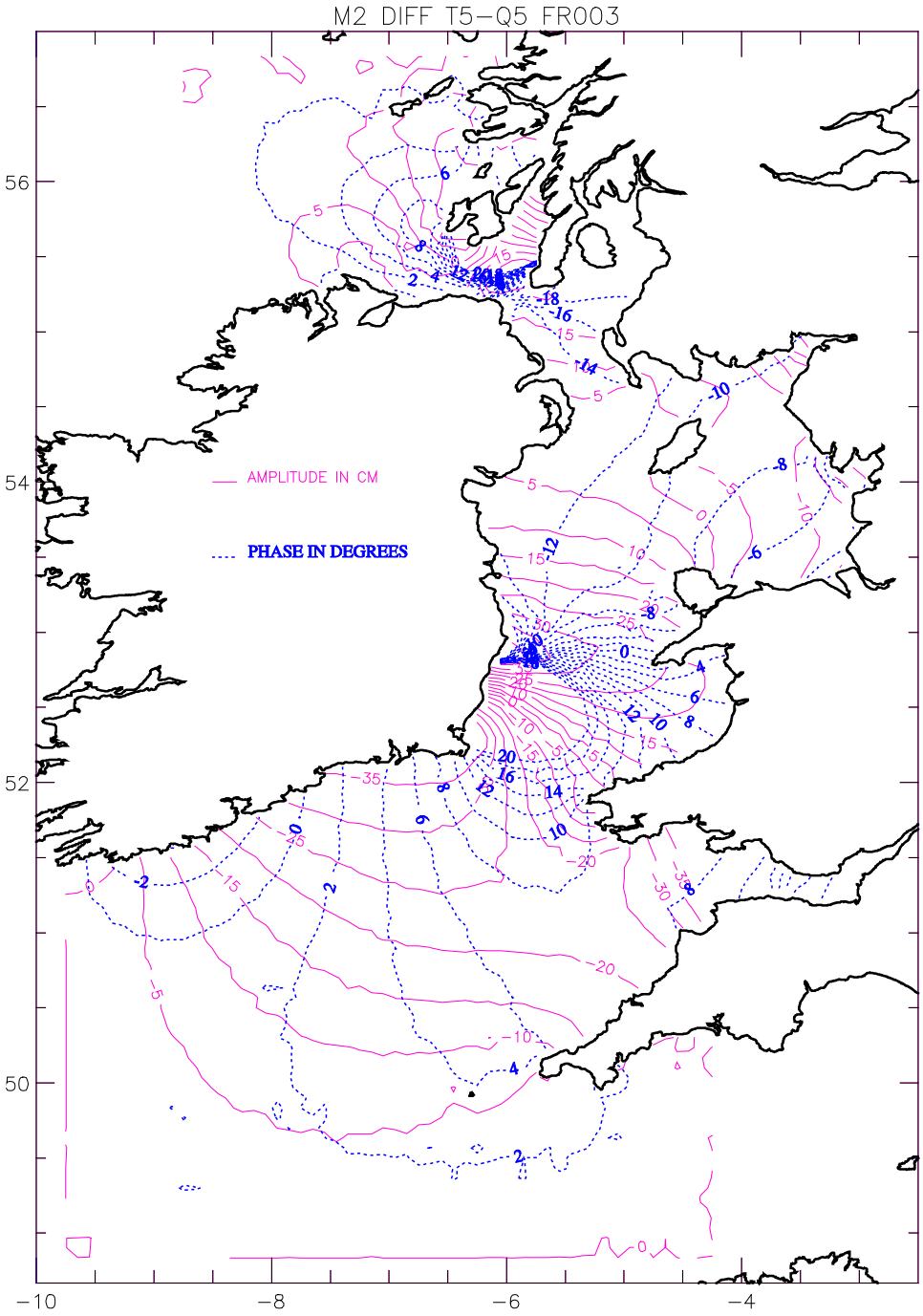
M2 DIFF T5−Q5 FR003
AMPLITUDE IN CM
PHASE IN DEGREES
56
54
52
50
−10
−8
−6
−4

Fig 8b:

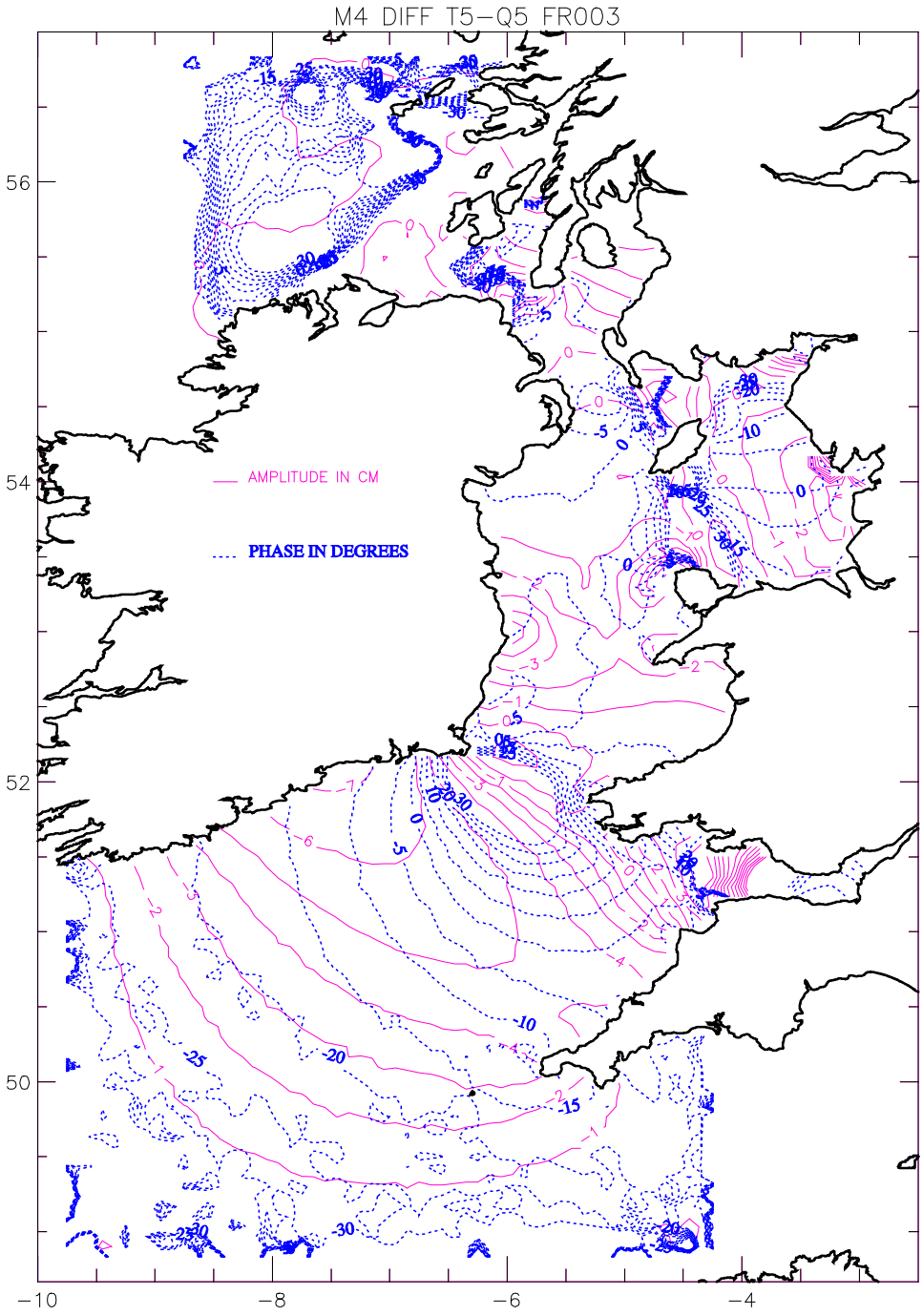
M4 DIFF T5−Q5 FR003
AMPLITUDE IN CM
PHASE IN DEGREES
56
54
52
50
−10
−8
−6
−4